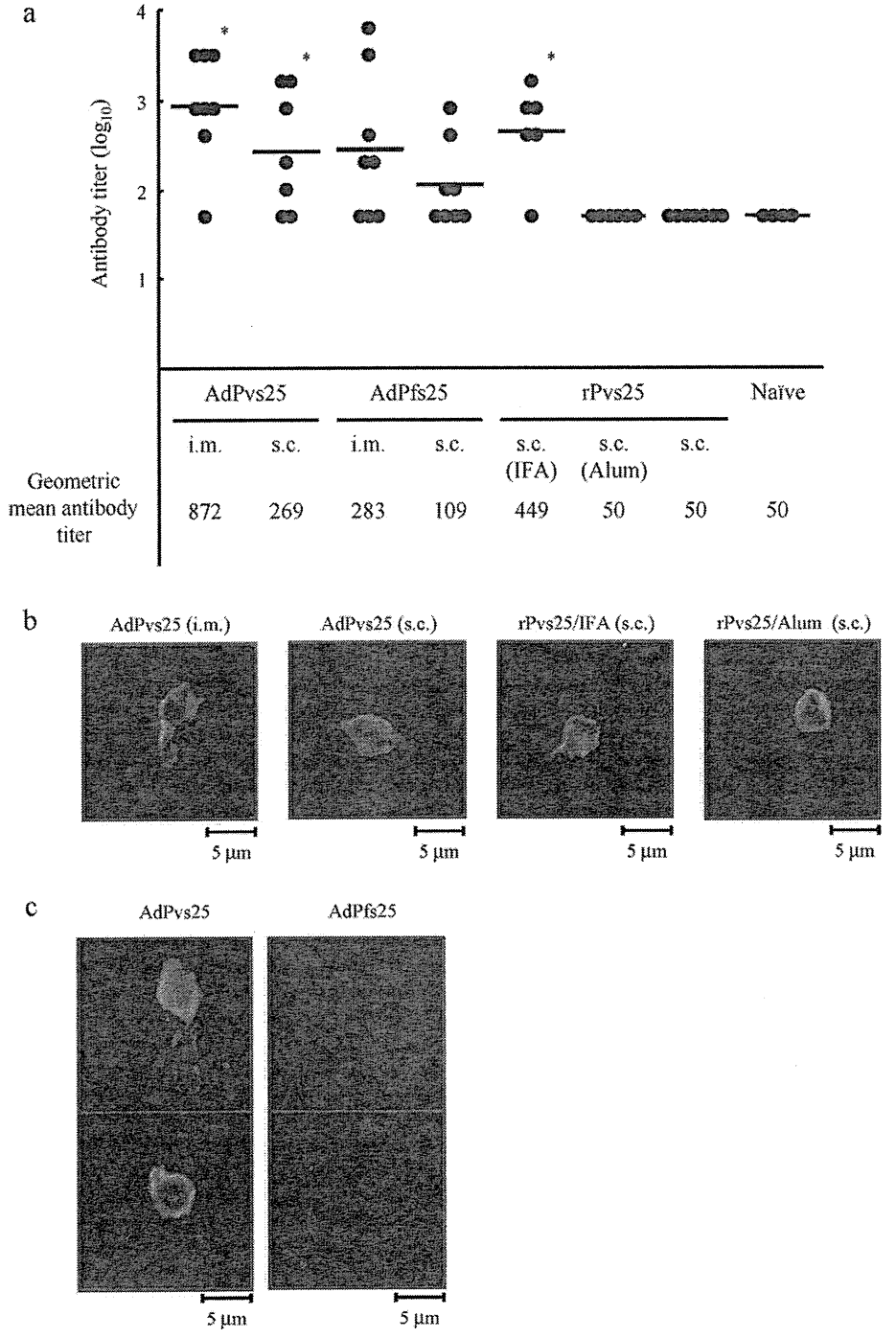

Fig. 1. Immunogenicity of AdPvs25 in mice. (a) Eight-week-old female BALB/c mice were immunized four times at weeks 0, 3, 5 and 7 *via* subcutaneous (s.c.) or intramuscular (i.m.) route with 5.1×10^8 plaque forming units of the AdPvs25, or three times at weeks 0, 2 and 4 *via* the s.c. route with 30 μg of recombinant Pvs25 (rPvs25) protein alone, or with incomplete Freund's adjuvant (IFA) or aluminum hydroxide (Alum), as controls. Serum samples were collected at week 8 or 6 for the adenovirus-vectored or the recombinant protein immunization, respectively, and evaluated for Pvs25-specific IgG titers. Serum from naïve mice was used as a negative control for the ELISA. Antibody titers were defined as the serum dilution that resulted in an OD_{415} of 0.1, or as the serum dilution where a one magnitude higher dilution gave an OD_{415} value less than 0.1. * indicates a significant difference to non-immune serum by the Wilcoxon–Mann–Whitney test ($P < 0.05$). (b) Ookinete-specific reactivity of the induced antisera as analyzed by immunofluorescence. The antisera derived from i.m. or s.c. immunization with the AdPvs25, or s.c. immunization with the rPvs25 protein emulsified with IFA or the rPvs25 protein mixed with Alum specifically recognized native Pvs25 protein expressed on the surface of *P. vivax* zygote/immature ookinetes. (c) The antisera derived from i.m. immunization with the AdPvs25 or the AdPfs25 were reacted to *P. vivax* zygote/immature ookinetes, indicating the specificity of the AdPvs25 antisera.

2.4. Detection of native Pvs25 using mouse antisera

Peripheral blood of *P. vivax*-infected volunteer patients was collected as described above. The gametocytemic blood was used to grow zygotes and ookinetes *in vitro* [32], then samples were spotted onto slides and fixed with acetone as described previously [27–30]. The slides were then blocked with 5% nonfat milk in PBS, and incubated with the mouse antiserum derived from immunization with

the AdPvs25, AdPfs25, or the rPvs25 protein emulsified with IFA, or the rPvs25 protein mixed with Alum, after diluting the antisera 100-fold with 5% nonfat milk in PBS. The samples were washed with ice-cold PBS and incubated with Alexa488-conjugated anti-mouse antibody (Invitrogen, Carlsbad, CA, USA). After washing with ice-cold PBS, slides were viewed by confocal scanning laser microscopy (LSM5 PASCAL; Carl Zeiss MicroImaging, Thornwood, NY, USA).

2.5. Statistical analysis

Statistical analyses were conducted by the Wilcoxon–Mann–Whitney test or the Kruskal–Wallis test using JMP software version 8.0 (SAS Institute, Inc., Cary, NC, USA).

3. Results and discussion

There is an increasing demand for the development of effective recombinant vaccine platform technologies to enhance vaccine efficacy by the innovation of new adjuvants or delivery systems [33]. This would seem to be particularly true for OSPs, because they are low-molecular-weight proteins that are by themselves not sufficiently immunogenic.

In this study, we engineered replication-defective human adenovirus serotype 5 for expression of a *P. vivax* OSP, Pvs25, to test its efficacy to induce transmission-blocking immunity. We immunized BALB/c mice through various routes including i.m., s.c., i.n. and i.g., and the Pvs25-specific serum IgG response was measured (Fig. 1a and Table 1). Parenteral (i.m. and s.c.) but not mucosal (i.n. and i.g.) immunization (Supplementary data Fig. 1) with the AdPvs25 induced robust IgG responses comparable in titers to those induced by the rPvs25 protein administered s.c. with IFA. Immunization by the i.m. route with the AdPvs25 tended to induce higher IgG response than s.c. immunization, and at least three booster injections seemed to be necessary to induce the maximal level of response (Supplementary data Fig. 1). AdPvs25-induced antisera could efficiently recognize the *P. vivax* ookinete surface as determined by the immunofluorescence assay (Fig. 1b). Although, rPvs25 protein immunization with aluminum hydroxide induced only a background level of IgG response as compared with the unimmunized naïve control serum (Fig. 1a), the induced antiserum could recognize the parasite surface as efficiently as the AdPvs25 or the rPvs25/IFA induced antiserum (Fig. 1b).

AdPfs25 immunization, particularly for the i.m. route, induced relatively high IgG response to the rPvs25 protein as determined by ELISA (Fig. 1a and Supplementary data Fig. 2), implicating that the induced antisera are somewhat cross-reactive at least at the recombinant protein level; however, the differences in IgG titers between AdPfs25 and the unimmunized naïve control groups did not reach statistically significant levels. Further, AdPfs25 antisera failed to react to the *P. vivax* ookinete (Fig. 1c), indicating the specificity of the AdPvs25 antisera.

Next, we evaluated the TBV efficacy of the induced mouse antisera against field isolates of *P. vivax* parasites in infected blood samples from volunteer patients in Thailand by the membrane feeding assay as described previously [28,29]. The same experiments were performed three times using blood samples from three different *P. vivax* (Pv)-infected volunteer donors (Pv-infected blood donors 1–3; Fig. 2a–c and Table 1). The average number of oocysts per mosquito fed on parasitized blood mixed with the antisera induced by parenteral immunization (i.m. or s.c.) with the AdPvs25 was reduced by 82–99% as compared with the unimmunized naïve control serum when parasite burden was low (Fig. 2a and b and Table 1). Although, the rPvs25/Alum induced no detectable Pvs25-specific serum IgG response (Fig. 1a and Table 1), its TBV efficacy (92–97% blockade; Fig. 2a and b and Table 1) was com-

Table 1
Summary of immunization experiments outlining antibody titers and transmission-blocking effects.

Immunization group	Immunization route	Adjuvant	Geometric mean antibody titer	TBV effect (Pv-infected blood donor 1)		TBV effect (Pv-infected blood donor 2)		TBV effect (Pv-infected blood donor 3)	
				Average oocyst number per mosquito (median oocyst number)	% Reduction in average oocyst number per mosquito (oocyst-free mosquitoes per 20 mosquitoes)	Average oocyst number per mosquito (median oocyst number)	% Reduction in average oocyst number per mosquito (oocyst-free mosquitoes per 20 mosquitoes)	Average oocyst number per mosquito (median oocyst number)	% Reduction in average oocyst number per mosquito (oocyst-free mosquitoes per 20 mosquitoes)
AdPvs25	i.m.	–	872§	1.5* (1.0)	82.3 (9)	0.1* (0)	98.6 (19)	10.0* (3.0)	71.4 (7)
	s.c.	–	269§	1.0* (0)	87.8 (11)	1.3* (0)	82.4 (13)	25.0 (14.5)	28.5 (1)
AdPfs25	i.m.	–	283	10.0 (7.0)	0 (4)	5.5 (5.0)	25.7 (3)	85.3 (71.5)	0 (0)
	s.c.	–	109	16.6 (18.0)	0 (1)	7.9 (6.0)	0 (1)	207.3 (206.0)	0 (0)
rPvs25	s.c.	IFA	449§	0* (0)	100 (20)	0* (0)	100 (20)	0* (0)	100 (20)
	s.c.	Alum	50	0.7* (0)	91.5 (13)	0.2* (0)	97.3 (17)	31.2 (24.5)	10.9 (1)
	s.c.	–	50	7.0 (6.0)	14.6 (1)	1.4* (0.5)	81.1 (10)	53.5 (34.0)	0 (1)
Naïve		–	50	8.2 (7.5)	0 (3)	7.4 (4.5)	0 (5)	35.0 (14.5)	0 (0)

i.m.: intramuscular; s.c.: subcutaneous; IFA: incomplete Freund's adjuvant; Alum: aluminum hydroxide; TBV: transmission-blocking vaccine; Pv: *Plasmodium vivax*.
* $P < 0.001$ *vs.* naïve.
§ $P < 0.005$ *vs.* naïve.
% Reduction is calculated as the reduction in the average oocyst number for each immunization group compared to the average oocyst number for the unimmunized naïve control group.

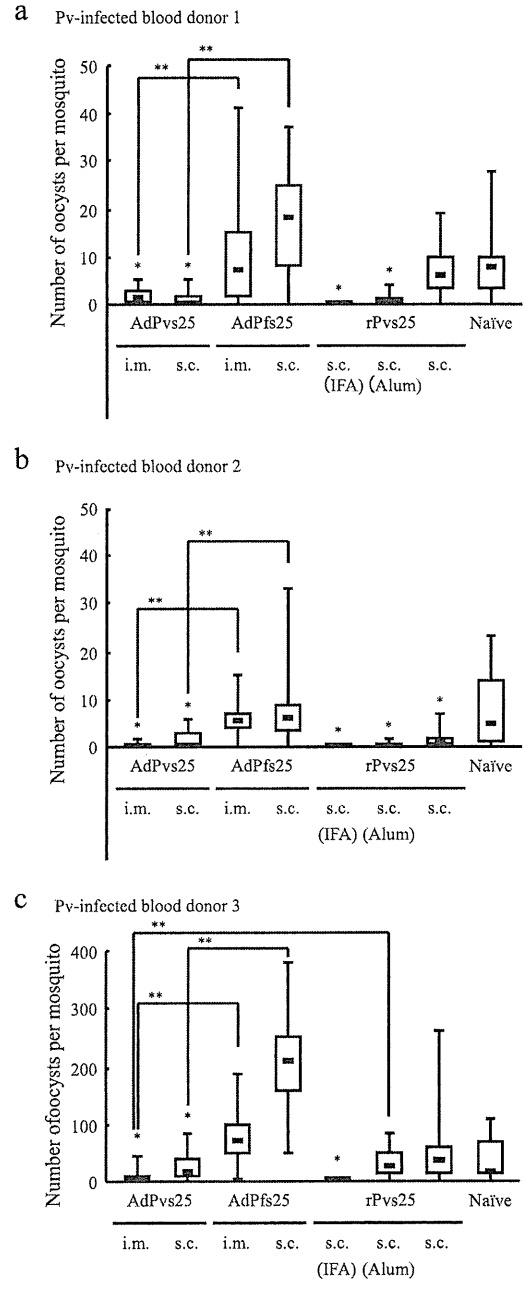

Fig. 2. Transmission-blocking effects induced by antisera (1/2 dilution) derived from mice immunized with the AdPvs25, the AdPfs25, or the rPvs25 protein were evaluated. The data were expressed as the median values of oocyst number per mosquito (black bar within the box) with 25% and 75% quartiles (box) and ranges (error bars). Three independent experiments were performed, using three blood samples from Pv-infected blood donors 1–3. * $P<0.001$ *vs.* naïve mice by the Wilcoxon–Mann–Whitney test; ** $P<0.001$ between the indicated two groups by the Wilcoxon–Mann–Whitney test.

parable to those attained by the AdPvs25. We do not know why the rPvs25/Alum immunization conferred substantial TBV efficacy without inducing antibody response detectable in ELISA (Fig. 1a); however, when the level of parasite burden increased as seen in the case for donor 3, the AdPvs25 appeared to become significantly more efficacious than the rPvs25/Alum, particularly for the i.m. immunization regimen (Fig. 2c and Table 1). These results suggest that adenovirus-vectored Pvs25 has potentially higher vaccine efficacy than the Alum-adjuvanted rPvs25 protein.

The rPvs25/IFA immunization consistently conferred a complete blockade regardless of the level of parasite burden; however, the local reactogenicity was considerably higher than Alum-adjuvanted or adenovirus-vectored immunization regimen.

Intraperitoneal or intravenous immunization with the AdPvs25 induced a robust serum IgG response, although its TBV effect was not assessed in this study. In contrast, despite the fact that adenoviruses mainly affect the respiratory system, the AdPvs25 administered by the i.n. route failed to induce a specific serum IgG response as determined by the ELISA (Supplementary Fig. 1). This might be due to the fact that only a low virus dose was able to be administered. However, the rPvs25 protein administered i.n. with a minute amount of cholera toxin (CT) adjuvant consistently induced a strong IgG response in mice, and as such its level of efficacy was very similar to that attained by the i.m. administered AdPvs25 immunization regimen (data not shown). Thus, it seems that adenovirus-vectored i.n. immunization is much less effective than the recombinant protein antigen administered through the same route with a potent mucosal adjuvant like CT. Administration through the i.g. route was also tested in this study, but failed to induce any antibody response, probably because the gastrointestinal environment is too destructive for the virus to effectively transduce the foreign gene. The intravaginal route was found to be another ineffective route to induce an antibody response by adenovirus immunization, and as such no specific serum IgG was observed. The reason for this failure might be the same as those for i.n. immunization.

In this study we concomitantly engineered a replication-defective adenovirus expressing Pfs25, an ortholog gene of Pvs25. Its immunization induced low but detectable cross-reactive serum IgG to the rPvs25 protein, although it did not reach a level of statistical significance as compared with the naïve control serum (Fig. 1a). However, the membrane feeding assay confirmed that no TBV effect was induced against *P. vivax* species (Fig. 2), suggesting that induction of interspecies cross-blocking immunity cannot be expected. However, a mixed administration of the two adenovirus vectors each expressing Pfs25 and Pvs25, or engineering of a single virus vector that co-expresses both P25 genes should be technically feasible, implicating that multi-species TBVs could be constructed. To address this possibility, we conducted a preliminary immunization experiment in which a mixture of the two adenoviruses, AdPfs25 and AdPvs25, were administered through various routes, and assessed immunogenicity towards both proteins. The results implicated that the existence of multiple viral vectors did not have a negative impact on the induction of specific IgG responses against the individual protein (data not shown).

Heterologous prime–boost regimens employing different viral vectors, different administration routes, or different vaccine formulations such as those using plasmid DNA or recombinant proteins, is thought to be a promising approach to enhance vaccine efficacy of malaria antigens [23,34–38]. To determine whether the prime–boost regimen is also applicable to OSP-based TBVs, we tested a DNA prime-adenovirus vector boost (one DNA injection and three consecutive adenovirus injections). The results implicated however that DNA immunization does not adequately replace adenovirus vector immunization, because the level of antibody remained lower than the adenovirus vector only immunization regimen (data not shown). Similarly, a combination of different immunization routes was evaluated and from our results, we concluded that replacement of parenteral with mucosal immunization induced a lower immune response (data not shown). Taken together, these results implicate that DNA or mucosal immunization, which was by itself found not to be sufficiently immunogenic, when combined with the parenteral adenovirus vector immunization, ablated to varying degrees the

overall vaccine efficacy. However, we were unable to make a final conclusive statement, at this preliminary stage of evaluation, regarding the suitability of a prime–boost regimen and whether or not it could be applied for TBVs. This is because there are other various possible combinations that need to be tested, such as an adenovirus prime–vaccinia virus boost regimen, which is known to be one of the most effective combinations [36,38].

Since OSP-based TBVs do not directly protect vaccinated individuals from infection, it should not be used as a "standalone" malaria vaccine. Researchers are beginning to realize that a single antigen, a single stage, or even a single species malaria vaccine developmental strategy can no longer be considered as a practical or realistic strategy, as was previously believed [5], and therefore a combination of heterologous immunization regimens, including the prime–boost method, need to be pursued more vigorously for future malaria vaccine development. In this sense, it is very feasible and should be technically possible to combine adenovirus-vectored TBVs with other virus vectored vaccines, such as vaccinia virus, or with viral vectors targeting the pre-erythrocytic or erythrocytic stages of single or multiple malaria species, or even in combination with vaccines targeting other infectious diseases.

Of course, there is still much scope for optimizing adenovirus-vectored OSP-based TBVs. For example, adenovirus serotype 5 used in the present study may need to be changed to other serotypes for future clinical application in malaria endemic areas in Africa, because a large proportion of African population has high serotype 5 antibody [37]. However, the present study should at least support the notion that malaria OSP antigens can be included in adenovirus-vectored or possibly other viral vectored immunization regimens, and that they are able to induce comparable levels of humoral immunity compared with those induced by the recombinant proteins combined with the Alum adjuvant.

Acknowledgments

We thank the staff of the Armed Forces Research Institute of Medical Sciences in Bangkok, Thailand, for their technical assistance. This work was supported by grants from the Program of Founding Research Centers for Emerging and Reemerging Infectious Diseases from The Ministry of Education, Culture, Sports, Science and Technology, Japan (MEXT); Grants-in-Aid for Scientific Research (19406009 and 20590425) and Scientific Research on Priority Areas (21022034) from MEXT; a grant from the Okinawa Industry Promotion Public Corporation; and the Cooperative Research Grant of the Institute of Tropical Medicine, Nagasaki University.

Appendix A. Supplementary data

Supplementary data associated with this article can be found, in the online version, at doi:10.1016/j.vaccine.2011.01.083.

References

[1] WHO. World Health Report. 2008.
[2] Greenwood BM, Fidock DA, Kyle DE, Kappe SH, Alonso PL, Collins FH, et al. Malaria: progress, perils, and prospects for eradication. J Clin Invest 2008;118(4 (April)):1266–76.
[3] Targett GA, Greenwood BM. Malaria vaccines and their potential role in the elimination of malaria. Malar J 2008;7(Suppl. 1):S10.
[4] Genton B. Malaria vaccines: a toy for travelers or a tool for eradication? Expert Rev Vaccines 2008;7(5 (July)):597–611.
[5] PATH malaria vaccine initiative: about the malaria vaccine roadmap. Available from: http://www.malariavaccineorg/malvac-roadmap.php.
[6] Sharma S, Pathak S. Malaria vaccine: a current perspective. J Vector Borne Dis 2008;45(1 (March)):1–20.
[7] WHO. Malaria vaccine rainbow tables. Available from: http://www.who.int/vaccine_research/links/Rainbow/en/index.html.
[8] Ballou WR. The development of the RTS, S malaria vaccine candidate: challenges and lessons. Parasite Immunol 2009;31(9 (September)):492–500.
[9] Richards JS, Beeson JG. The future for blood-stage vaccines against malaria. Immunol Cell Biol 2009;87(5 (July)):377–90.
[10] Tsuboi T, Tachibana M, Kaneko O, Torii M. Transmission-blocking vaccine of *vivax* malaria. Parasitol Int 2003;52(1 (March)):1–11.
[11] Kaslow DC. Transmission-blocking vaccines: uses and current status of development. Int J Parasitol 1997;27(2 (February)):183–9.
[12] Carter R. Transmission blocking malaria vaccines. Vaccine 2001;19(17–19 (March)):2309–14.
[13] Arevalo-Herrera M, Chitnis C, Herrera S. Current status of *Plasmodium vivax* vaccine. Hum Vaccin 2010;6(1 (January)).
[14] Birkett AJ. PATH malaria vaccine initiative (MVI): perspectives on the status of malaria vaccine development. Hum vaccin 2010;6(1 (January)):139–45.
[15] Sina B. Focus on *Plasmodium vivax*. Trends Parasitol 2002;18(7 (July)):287–9.
[16] Kochar DK, Das A, Kochar SK, Saxena V, Sirohi P, Garg S, et al. Severe *Plasmodium vivax* malaria: a report on serial cases from Bikaner in northwestern India. Am J Trop Med Hyg 2009;80(2 (February)):194–8.
[17] Bill and Melinda Foundation. Global Health Program. Available from: http://www.gatesfoundation.org/global-health/Documents/malaria-strategy.pdf.
[18] Herrington DA, Nardin EH, Losonsky G, Bathurst IC, Barr PJ, Hollingdale MR, et al. Safety and immunogenicity of a recombinant sporozoite malaria vaccine against *Plasmodium vivax*. Am J Trop Med Hyg 1991;45(6 (December)):695–701.
[19] Malkin EM, Durbin AP, Diemert DJ, Sattabongkot J, Wu Y, Miura K, et al. Phase 1 vaccine trial of Pvs25H: a transmission blocking vaccine for *Plasmodium vivax* malaria. Vaccine 2005;23(24 (May)):3131–8.
[20] Wu Y, Ellis RD, Shaffer D, Fontes E, Malkin EM, Mahanty S, et al. Phase 1 trial of malaria transmission blocking vaccine candidates Pfs25 and Pvs25 formulated with montanide ISA 51. PLoS ONE 2008;3(7):e2636.
[21] Li S, Locke E, Bruder J, Clarke D, Doolan DL, Havenga MJ, et al. Viral vectors for malaria vaccine development. Vaccine 2007;25(14 (March)):2567–74.
[22] Draper SJ, Heeney JL. Viruses as vaccine vectors for infectious diseases and cancer. Nat Rev Microbiol 2010;8(1 (January)):62–73.
[23] Limbach KJ, Richie TL. Viral vectors in malaria vaccine development. Parasite Immunol 2009;31(9 (September)):501–19.
[24] Reyes-Sandoval A, Harty JT, Todryk SM. Viral vector vaccines make memory T cells against malaria. Immunology 2007;121(2 (June)):158–65.
[25] Beeson JG, Osier FH, Engwerda CR. Recent insights into humoral and cellular immune responses against malaria. Trends Parasitol 2008;24(12 (December)):578–84.
[26] Russell KL, Hawksworth AW, Ryan MA, Strickler J, Irvine M, Hansen CJ, et al. Vaccine-preventable adenoviral respiratory illness in US military recruits, 1999–2004. Vaccine 2006;24(15 (April)):2835–42.
[27] Miyata T, Harakuni T, Tsuboi T, Sattabongkot J, Kohama H, Tachibana M, et al. *Plasmodium vivax* ookinete surface protein, Pvs25, linked to cholera toxin B subunit induces potent transmission-blocking immunity by intranasal as well as subcutaneous immunization. Infect Immun 2010.
[28] Arakawa T, Komesu A, Otsuki H, Sattabongkot J, Udomsangpetch R, Matsumoto Y, et al. Nasal immunization with a malaria transmission-blocking vaccine candidate, Pfs25, induces complete protective immunity in mice against field isolates of *Plasmodium falciparum*. Infect Immun 2005;73(11 (November)):7375–80.
[29] Arakawa T, Tsuboi T, Kishimoto A, Sattabongkot J, Suwanabun N, Rungruang T, et al. Serum antibodies induced by intranasal immunization of mice with *Plasmodium vivax* Pvs25 co-administered with cholera toxin completely block parasite transmission to mosquitoes. Vaccine 2003;21(23 (July)):3143–8.
[30] Arakawa T, Tachibana M, Miyata T, Harakuni T, Kohama H, Matsumoto Y, et al. Malaria ookinete surface protein-based vaccination via the intranasal route completely blocks parasite transmission in both passive and active vaccination regimens in a rodent model of malaria infection. Infect Immun 2009;77(12 (December)):5496–500.
[31] Kass-Eisler A, Li K, Leinwand LA. Prospects for gene therapy with direct injection of polynucleotides. Ann NY Acad Sci 1995;772(November):232–40.
[32] Suwanabun N, Sattabongkot J, Tsuboi T, Torii M, Maneechai N, Rachapaew N, et al. Development of a method for the in vitro production of *Plasmodium vivax* ookinetes. J Parasitol 2001;87(4 (August)):928–30.
[33] O'Hagan DT, Valiante NM. Recent advances in the discovery and delivery of vaccine adjuvants. Nat Rev Drug Discov 2003;2(9 (September)):727–35.
[34] Kongkasuriyachai D, Bartels-Andrews L, Stowers A, Collins WE, Sullivan J, Sattabongkot J, et al. Potent immunogenicity of DNA vaccines encoding *Plasmodium vivax* transmission-blocking vaccine candidates Pvs25 and Pvs28-evaluation of homologous and heterologous antigen-delivery prime–boost strategy. Vaccine 2004;22(23–24 (August)):3205–13.
[35] Coban C, Philipp MT, Purcell JE, Keister DB, Okulate M, Martin DS, et al. Induction of *Plasmodium falciparum* transmission-blocking antibodies in nonhuman primates by a combination of DNA and protein immunizations. Infect Immun 2004;72(1 (January)):253–9.
[36] Reyes-Sandoval A, Berthoud T, Alder N, Siani L, Gilbert SC, Nicosia A, et al. Prime–boost immunization with adenoviral and modified vaccinia virus Ankara vectors enhances the durability and polyfunctionality of pro-

tective malaria CD8+ T-cell responses. Infect Immun 2010;78(1 (January)): 145–53.
[37] Hill AV, Reyes-Sandoval A, O'Hara G, Ewer K, Lawrie A, Goodman A, et al. Prime–boost vectored malaria vaccines: progress and prospects. Hum vaccin 2010;6(1 (January)).
[38] Bruna-Romero O, Gonzalez-Aseguinolaza G, Hafalla JC, Tsuji M, Nussenzweig RS. Complete, long-lasting protection against malaria of mice primed and boosted with two distinct viral vectors expressing the same plasmodial antigen. Proc Natl Acad Sci USA 2001;98(20 (September)):11491–6.

Parasitology International 60 (2011) 132–138

Contents lists available at ScienceDirect

Parasitology International

journal homepage: www.elsevier.com/locate/parint

Plasmodial ortholog of *Toxoplasma gondii* rhoptry neck protein 3 is localized to the rhoptry body

Daisuke Ito [a], Eun-Taek Han [b], Satoru Takeo [a], Amporn Thongkukiatkul [c], Hitoshi Otsuki [d], Motomi Torii [e], Takafumi Tsuboi [a,f,*]

[a] Cell-Free Science and Technology Research Center, Ehime University, Matsuyama, Ehime 790-8577, Japan
[b] Department of Parasitology, Kangwon National University College of Medicine, Chuncheon, Republic of Korea
[c] Department of Biology, Faculty of Science, Burapha University, Chonburi 20131, Thailand
[d] Division of Medical Zoology, Faculty of Medicine, Tottori University, Yonago, Tottori 683-8503, Japan
[e] Department of Molecular Parasitology, Ehime University Graduate School of Medicine, Shitsukawa, Toon, Ehime 791-0295, Japan
[f] Venture Business Laboratory, Ehime University, Matsuyama, Ehime 790-8577, Japan

ARTICLE INFO

Article history:
Received 23 November 2010
Received in revised form 24 December 2010
Accepted 7 January 2011
Available online 13 January 2011

Keywords:
Cell-free expression
Erythrocyte invasion
Merozoite
Plasmodium falciparum
Rhoptry

ABSTRACT

The proteins in apical organelles of *Plasmodium falciparum* merozoite play an important role in invasion into erythrocytes. Several rhoptry neck (RON) proteins have been identified in rhoptry proteome of the closely-related apicomplexan parasite, *Toxoplasma gondii*. Recently, three of *P. falciparum* proteins orthologous to *TgRON* proteins, *Pf*RON2, 4 and 5, were found to be located in the rhoptry neck and interact with the micronemal protein apical membrane antigen 1 (*Pf*AMA1) to form a moving junction complex that helps the invasion of merozoite into erythrocyte. However, the other *P. falciparum* RON proteins have yet to be characterized. Here, we determined that "PFL2505c" (hereafter referred to as *pfron3*) is the ortholog of the *tgron3* in *P. falciparum* and characterized its protein expression profile, subcellular localization, and complex formation. Protein expression analysis revealed that *Pf*RON3 was expressed primarily in late schizont stage parasites. Immunofluorescence microscopy (IFA) showed that *Pf*RON3 localizes in the apical region of *P. falciparum* merozoites. Results from immunoelectron microscopy, along with IFA, clarified that *Pf*RON3 localizes in the rhoptry body and not in the rhoptry neck. Even after erythrocyte invasion, *Pf*RON3 was still detectable at the parasite ring stage in the parasitophorous vacuole. Moreover, co-immunoprecipitation studies indicated that *Pf*RON3 interacts with *Pf*RON2 and *Pf*RON4, but not with *Pf*AMA1. These results suggest that *Pf*RON3 partakes in the novel *Pf*RON complex formation (*Pf*RON2, 3, and 4), but not in the moving junction complex (*Pf*RON2, 4, 5, and *Pf*AMA1). The novel *Pf*RON complex, as well as the moving junction complex, might play a fundamental role in erythrocyte invasion by merozoite stage parasites.

1. Introduction

Malaria is caused by the replication of protozoan parasites of the genus *Plasmodium* in circulating host erythrocytes [1]. The invasion process of merozoite stage parasite into erythrocyte requires the discharge of contents of apical secretory organelles (micronemes and rhoptries) to form an irreversible contact, called a tight junction, between the merozoite and the erythrocyte membrane. This tight junction migrates from the anterior to posterior poles of the merozoite. According to this moving junction, the host membrane invaginates the merozoites to eventually form a parasitophorous vacuole [2,3]. The moving junction is one of the most distinctive features of apicomplexan invasion into host cells, and was first observed in *Plasmodium* species [4]. Studies in apicomplexan parasite *Toxoplasma gondii* identified a total of four proteins from distinct apical secretory organelles to form a moving junction complex; micronemal protein apical membrane antigen 1 (AMA1) and three rhoptry neck (RON) proteins, RON2, RON4, and RON5 [5,6]. Recently, this RON–AMA1 complex (*Pf*RON2, *Pf*RON4, *Pf*RON5, and *Pf*AMA1) was also identified in *Plasmodium falciparum* [7–9]. Attempts to knockout the AMA1 gene locus were unsuccessful in both *Plasmodium* [10] and *T. gondii* [11]. AMA1-binding peptide R1 not only prevents RON–AMA1 complex interaction, but also blocks *P. falciparum* merozoite invasion into erythrocytes [9].

Although the cumulative evidence above strongly suggests that the conserved RON–AMA1 complex plays an essential role in merozoite invasion, it is yet to be clarified whether molecules other than RON2, RON 4, and RON 5, play roles in the formation of the moving junction complex and in the invasion process. The report on *T. gondii* rhoptry proteome identified the presence of other RON proteins, RON1 and RON3 [12]. Therefore, we were interested in

* Corresponding author. Cell-Free Science and Technology Research Center, Ehime University, Matsuyama, Ehime 790-8577, Japan. Tel.: +81 89 927 8277; fax: +81 89 927 9941.
E-mail address: tsuboi@ccr.ehime-u.ac.jp (T. Tsuboi).

1383-5769/$ – see front matter © 2011 Elsevier Ireland Ltd. All rights reserved.
doi:10.1016/j.parint.2011.01.001

identifying the ortholog of *tgron3* in *P. falciparum* and in characterizing its protein expression profile, subcellular localization, and role in the formation of the RON–AMA1 complex.

2. Materials and methods

2.1. Parasites

P. falciparum asexual stages (3D7 strain) were maintained in human erythrocytes (blood group O^+) *in vitro*, as previously described [13].

2.2. RNA isolation and cDNA synthesis

Total RNA was extracted from *P. falciparum* schizont-infected erythrocytes (purified by differential centrifugation on a 70%/40% Percoll/sorbitol gradient) using the TRizol Reagent (Invitrogen, Carlsbad, CA). Following DNase treatment, cDNA was generated with a random hexamer using the SuperScriptIII® First Strand Synthesis System (Invitrogen).

2.3. Antibodies

Recombinant *Pf*RON3 proteins were produced using the wheat germ cell-free translation system (CellFree Sciences, Matsuyama, Japan) as described previously [14–16]. Briefly, regions of the *Pf*RON3 gene encoding the deduced amino acid sequence, 927–1056 (*Pf*RON3_1) and 1686–1884 (*Pf*RON3_2), were PCR-amplified from *P. falciparum* 3D7 blood-stage cDNA and ligated into pEU-E01-GST-(TEV)-N2 (CellFree Sciences), an expression plasmid with an N-terminal glutathione S transferase (GST)-tag followed by a tobacco etch virus (TEV) protease cleavage site, designed specifically for the wheat germ cell-free protein expression. Oligonucleotide primers used in the PCR amplification were *Pf*RON3_XhoIF1 (5′-ctcgagGATATTCCATTAAAAGAAACCTATAAATT-3′) and *Pf*RON3_BamHIR1 (5′-ggatccCTAATGTGGGAACATTTCATGATTTGGTA-3′) for *Pf*RON3_1, and *Pf*RON3_XhoIF2 (5′-ctcgagGATTTTAAAGATAAATCAGATGATGATC-3′) and *Pf*RON3_BamHIR2 (5′-ggatccCTATTTTTTAGGTACATATATATTATATGGTC-3′) for *Pf*RON3_2 (XhoI and BamHI restriction sites are underlined). Both GST-*Pf*RON3_1 and GST-*Pf*RON3_2 were captured using a glutathione-Sepharose 4B column (GE Healthcare, Camarillo, CA), and eluted by on-column cleavage with 60 U of AcTEV protease (Invitrogen) after extensive washing with PBS. To generate anti-*Pf*RON3_1 and anti-*Pf*RON3_2 sera, female BALB/c mice were immunized subcutaneously with 20μg of purified *Pf*RON3_1 or *Pf*RON3_2 emulsified with Freund's adjuvant. A Japanese white rabbit was also immunized subcutaneously with 250μg of purified *Pf*RON3_1 or *Pf*RON3_2 emulsified with Freund's adjuvant. All immunizations were performed 3 times at 3-week intervals, and then antisera were collected 2 weeks after the third immunization. In a similar manner, mouse anti-*Pf*RAP1 (aa 1–782) antibody, mouse anti-*Pf*EXP2 (aa 25–287) antibody, mouse and rabbit anti-*Pf*AMA1 (aa 25–546) antibodies, and rabbit anti-GST antibody, were generated as control. Rabbit antisera against the *Pf*RON3_1 and *Pf*RON3_2 proteins were affinity purified using a column conjugated with recombinant *Pf*RON3_1 or *Pf*RON3_2 as ligands, respectively. Briefly, recombinant *Pf*RON3_1 or *Pf*RON3_2 was covalently linked to a HiTrap™ NHS-activated HP column (GE Healthcare) as manufacturer's recommendation. Rabbit antiserum was then applied to either the *Pf*RON3_1- or the *Pf*RON3_2-conjugated column. After an extensive washing step with 20 mM phosphate buffer (pH 7.0), antigen-specific IgGs were eluted with 0.1 M glycine–HCl (pH 2.5), and then immediately neutralized with 1 M Tris (pH 9.0). Mouse monoclonal anti-*Pf*RON4 antibody (26C64F12) [7] and anti-*Pf*RESA antibody (23/9) [17] were kind gifts from Jean F. Dubremetz (Université de Montpellier 2, France) and Robin F. Anders (La Trobe University, Australia), respectively.

2.4. SDS-PAGE and western blot analysis

P. falciparum cultured parasites were harvested after tetanolysin (List Biological Laboratories, Inc., Campbell, CA) treatment that can remove the hemoglobin without loss of parasite proteins present in the parasitophorous vacuolar space [18]. The parasite proteins were then extracted in SDS-PAGE loading buffer, incubated at 4 °C for 6 h, and subjected to electrophoresis under reducing condition on a 12.5% polyacrylamide gel (ATTO, Tokyo, Japan). Proteins were then transferred to a 0.2-μm PVDF membrane (GE Healthcare). The proteins were immunostained with antisera followed by horseradish peroxidase-conjugated secondary antibody (GE Healthcare) and visualized with Immobilon Western Chemiluminescent HRP Substrate (Millipore, Billerica, MA) on a LAS 4000 mini luminescent image analyzer (GE Healthcare). The relative molecular masses of the proteins were estimated with reference to Precision Plus Protein Standards (BioRad, Hercules, CA).

2.5. Immunoprecipitation

Immunoprecipitation was carried out as previously described [19]. Briefly, proteins were extracted from late schizont parasite pellets in PBS with 1% Triton X-100 containing Complete Proteinase Inhibitor Cocktail (Roche, Indianapolis, IN). Supernatants (50 μl) were pre-incubated at 4 °C for 1 h with 40 μl of 50% protein G-conjugated beads (GammaBind Plus Sepharose; GE Healthcare) in NETT buffer (50 mM Tris–HCl, 0.15 M NaCl, 1 mM EDTA, and 0.5% Triton X-100) supplemented with 0.5% BSA (fraction V; Sigma-Aldrich Corporation, St. Louis, MO). Aliquots of recovered supernatants were incubated either with rabbit anti-*Pf*RON3_1, anti-*Pf*AMA1, anti-*Pf*RON2, or anti-GST antibody, and then 40 μl of 50% protein G-conjugated bead suspension was added. After one-hour incubation at 4 °C, the beads were washed once with NETT–0.5% BSA, once with NETT, once with high-salt NETT (0.5 M NaCl), once with NETT, and once with low-salt NETT (0.05 M NaCl and 0.17% Triton X-100). Finally, proteins were eluted from the protein G-conjugated beads with 0.1 M glycine–HCl (pH 2.5), and then immediately neutralized with 1 M Tris pH 9.0. The supernatants were used for western blot analysis.

2.6. Indirect immunofluorescence assay

Thin smears of ring or schizont-enriched *P. falciparum*-infected erythrocytes were prepared on glass slides and stored at −80 °C. The smears were thawed, fixed with 4% formaldehyde at room temperature for 10 min, permeabilized with PBS containing 0.1% Triton X-100 at room temperature for 15 min, and blocked with PBS containing 5% non-fat milk at 37 °C for 30 min. The smears were then incubated with rabbit anti-*Pf*RON3 antibodies (1:500 dilution) and control mouse antibodies at 37 °C for 1 h, followed by incubation with both Alexa Fluor 488-conjugated goat anti-rabbit IgG and Alexa Fluor 546-conjugated goat anti-mouse IgG (Invitrogen) as secondary antibodies (1:500) at 37 °C for 30 min. Nuclei were stained with 4′,6-diamidino-2-phenylindole (2 μg/ml, DAPI) mixed with a secondary antibody solution. Slides were mounted in ProLong Gold Antifade reagent (Invitrogen) and viewed under ×63 oil-immersion lens. High-resolution image-capture and processing were performed using a confocal scanning laser microscope (LSM5 PASCAL or LSM710; Carl Zeiss MicroImaging, Thornwood, NY). Images were processed in Adobe Photoshop (Adobe Systems Inc., San José, CA).

2.7. Immunoelectron microscopy

Parasites were fixed for 15 min on ice in a mixture of 1% paraformaldehyde and 0.1% glutaraldehyde in 0.1 M phosphate buffer (pH 7.4). Fixed specimens were washed, dehydrated, and embedded in LR White resin (Polysciences, Inc., Warrington, PA) as previously

have been described [20,21]. Ultrathin sections were blocked in PBS containing 5% non-fat milk and 0.01% Tween 20 (PBS-MT) at 37 °C for 30 min. Grids were then incubated at 4 °C overnight with rabbit anti-*Pf*RON3_2 or control sera in PBS-MT (1:20). After washing with PBS containing 10% BlockAce (Yukijirushi, Sapporo, Japan) and 0.01% Tween 20 (PBS-BT), the grids were incubated at 37 °C for 1 h with goat anti-rabbit IgG conjugated to 10 nm gold particles (GE Healthcare) diluted 1:20 in PBS-MT, rinsed with PBS-BT, and fixed at room temperature for 10 min in 2.5% glutaraldehyde to stabilize the gold particles. The grids were then rinsed with distilled water, dried, and stained with uranyl acetate and lead citrate. Samples were examined with a transmission electron microscope (JEM-1230; JEOL, Tokyo, Japan).

3. Results

3.1. Primary structure analysis of the RON3 orthologs

Using *Tg*RON3 (TGME49_023920) as a query in BLAST analyses [22], we found RON3 orthologs in *P. falciparum* (*Pf*RON3; PFL2505c, PlasmoDB) [23], *P. yoelii* 17XNL strain (*Py*RON3; PY01808, PlasmoDB), *P. vivax* Sal-I strain (*Pv*RON3; PVX_101485, PlasmoDB), *P. knowlesi* H strain (*Pk*RON3; PKH_146960, PlasmoDB), *P. chabaudi* AS strain (*Pch*RON3; PCA_146710, PlasmoDB), *P. berghei* ANKA strain (*Pb*RON3; PBANKA_146490, PlasmoDB), and *Eimeria tenella* (*Et*RON3; CAO79912, Sanger Institute). The full-length *Pf*RON3 protein consists of 2215 amino acid residues, with a putative N-terminal signal peptide sequence predicted by SignslP3.0 [24] to span amino acid residues 1 – 22. Three transmembrane regions (TM) (aa 250–272, 276–298, and 551–573) were predicted by TMHMM2.0 [25], and one coiled coil region (aa 1822–1847) was predicted by SMART [26]. Alignment of the deduced amino acid sequences of all the RON3 orthologs among the genus *Plasmodium* using Clustal W [27] demonstrated that twelve Cys residues are conserved (Fig. 1), with a 42% overall sequence identity. Moreover, the N-terminal region is highly conserved among the RON3 orthologs in the genus *Plasmodium*, in *T. gondii*, and in *E. tenella* (Fig. 2).

3.2. PfRON3 is expressed in the schizont stage and existed in the ring stage

The PfRON3 protein expression profile was analyzed by stage-specific western blot analysis using tightly synchronized parasites as antigens. Both antibodies (α-*Pf*RON3_1 and _2) recognized a band slightly larger than 250 kDa corresponding to the predicted molecular mass of *Pf*RON3 in late stage parasites, 40–44 h post invasion (Fig. 3A, arrowhead). Furthermore, both antibodies also recognized a prominent 190-kDa band, 40–44 h post invasion (Fig. 3A, arrow). After erythrocyte invasion, the 190-kDa band quickly degraded to 50- and 40-kDa bands (Figs. 3A and 4H). However, a small amount of the 190-kDa band was present throughout the ring (Figs. 3A and 4H) and trophozoite stages (Fig. 3A, 24–36 h). Additionally, only the anti-*Pf*RON3_2 antibody recognized a 37-kDa band, 40–44 h post invasion that might represent one of the processed forms of the *Pf*RON3 protein (Fig. 3A). Neither anti-PfRON3_1 or -PfRON3_2 had any reactivity against antigens of uninfected erythrocytes (Supplementary Fig. S1).

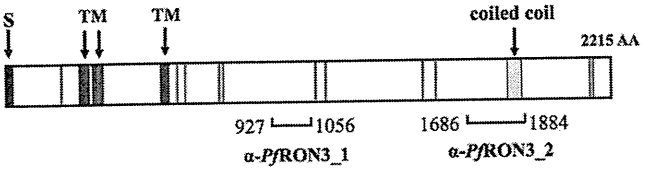

Fig. 1. Schematic representation of *Pf*RON3. The primary structure of *Pf*RON3 is depicted based on the analyses described in the Results section. S and TM indicate putative signal peptide (black) and transmembrane (blue) sequences, respectively. The yellow color box indicates a coiled coil region. Vertical red bars indicate conserved Cys residues in orthologs among the genus *Plasmodium*. The regions used to generate anti-*Pf*RON3 sera (α-*Pf*RON3_1 and α-*Pf*RON3_2) are indicated.

3.3. PfRON3 localizes in the rhoptry body of merozoites

In order to determine the sub cellular localization of *Pf*RON3, a dual label indirect immunofluorescence assay (IFA) was performed using anti-*Pf*RON3_2 antibody with anti-*Pf*RAP1 (rhoptry body marker), anti-*Pf*RON2 (rhoptry neck marker), anti-*Pf*AMA1 (microneme marker), and anti-*Pf*RESA (dense granule marker) antibodies as controls (Fig. 4). In mature schizonts, the anti-*Pf*RON3 antibody produced a punctate pattern of fluorescence in the apical end of each developing merozoite. Although some of the *Pf*RON3 signals overlapped with those of *Pf*RON2, *Pf*AMA1, or *Pf*RESA the *Pf*RON3 signals did not completely colocalize with those of the controls, whereas complete colocalization was observed between the signals of PfRON3 and *Pf*RAP1. Negative control sera were always used and these images were found to be negative (data not shown). To confirm the IFA results, the precise subcellular localization of *Pf*RON3 in the merozoite. Using anti-*Pf*RON3 antibody, gold particle signals were detected in the body portion of the rhoptries (Fig. 5).

3.4. PfRON3 is found in the parasitophorous vacuolar space after merozoite invasion into erythrocyte

To investigate *Pf*RON3 localization after the parasite invades erythrocytes, we performed IFA on ring stage parasites. *Pf*RAP1 and *Pf*EXP2 were used as parasitophorous vacuolar (PV) markers because they have been demonstrated to be present in ring stages and to associate with the PV [28–30]. We found that *Pf*RON3 colocalized with the PV markers, *Pf*RAP1 and *Pf*EXP2 in a discrete compartment surrounding the ring stage parasites (Fig. 6A). Next we performed western blot analysis using extracts of tightly synchronized ring or schizont stage parasites (Fig. 6B). *Pf*RON3 was detected in ring and schizont stage parasites together with *Pf*RAP1 and *Pf*EXP2. However *Pf*RON2 and *Pf*RON4 were detected only in schizont stage parasites (Fig. 6B) in agreement with the IFA results (Fig. 6A). Negative control sera were always used and these images were found to be negative (data not shown).

3.5. PfRON3 forms a complex with PfRON2 and PfRON4, but not with PfAMA1

To evaluate the interaction between *Pf*RON3 and the RON–AMA1 complex, we performed immunoprecipitation experiments using mature schizont-rich parasite extracts (Fig. 7). We did not detect *Pf*RON3 in the immunoprecipitate obtained using anti-*Pf*AMA1 antibody. However, PfRON3 was found in the anti-*Pf*RON2 precipitates. In the reciprocal experiment, *Pf*RON2 and *Pf*RON4 were detected in the immunoprecipitate obtained using the anti-*Pf*RON3_1 antibody; however, *Pf*AMA1 was not detected (Fig. 7). There was negligible crossreactivity between the anti-PfRON3_1 or anti-PfRON3_2 IgGs and PfRON2 and PfRON4 (Supplementary Fig. S1). These faint crossreactions were insignificant compared to the reactions with the actual target molecules.

4. Discussion

In this study, we characterized the protein expression profile and subcellular localization of *P. falciparum* RON3 as well as its complex formation with *Pf*RON2 and *Pf*RON4.

Studies of the apicomplexan parasite *T. gondii* identified various *Tg*RON proteins (RON2, RON4, RON5 [5,6], RON1, and RON3 [12]). The potential orthologs of the *Tg*RON proteins were subsequently

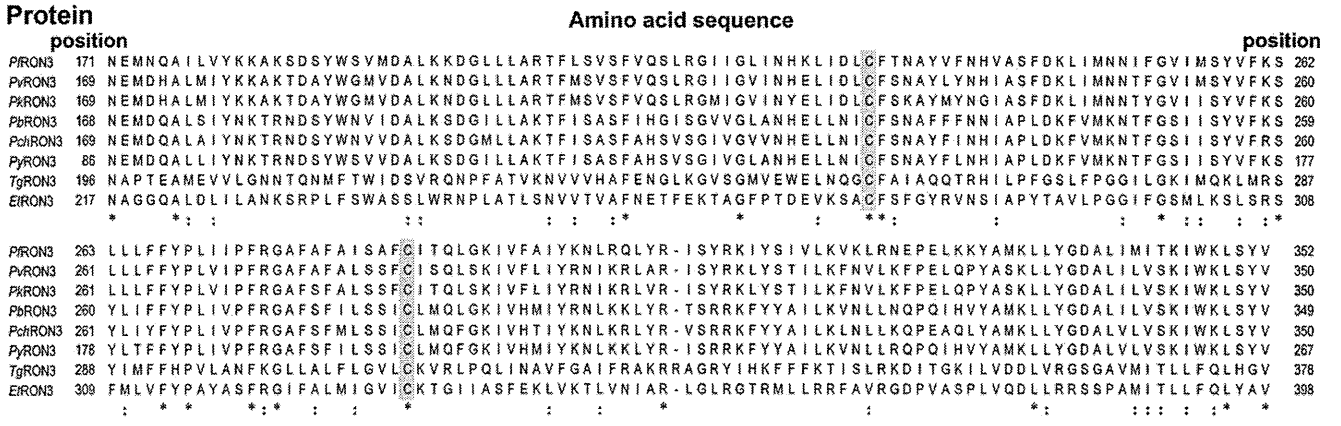

Fig. 2. Amino acid alignment of the conserved N-terminal region of RON3 orthologs. Deduced amino acid sequences of RON3 orthologs were aligned using Clustal W with manual correction. "*" indicates the conserved residues in the aligned sequences. ":" indicates conservative substitutions. Cys residues are highlighted in yellow.

identified in *P. falciparum*. Bradley et al. [12] suggested that *Pf*RON3 (PFL2505c) is an ortholog of *Tg*RON3 (TGME49_023920). However, Proellocks et al. [31] analyzed the amino acid sequence similarities of the RON orthologs identified in the genera *Plasmodium, Toxoplasma,* and some (but not all) *Apicomplexa*, and reported that, they may not be true orthologs because the collective sequence identity is below 12% [31]. In contrast, our pair-wise amino acid alignments between *T. gondii* and *P. falciparum* RON orthologs showed 11% identity between RON1 orthologs (TGME49_110010 vs. PFD0207c), 14% between RON2 orthologs(TGME49_100100 vs. PF14_0495), 12% between RON3 orthologs (TGME49_023920 vs. PFL2505c), and 10% between RON4 orthologs (TGME49_029010 vs. PF11_0168), suggesting that the amino acid identity between RON3 orthologs (*Tg*RON3 and *Pf*RON3) is comparable to that of other RON orthologs. Furthermore, multiple alignments of the deduced amino acid sequences of apicomplexan parasite RON3 orthologs showed that the N-terminal regions are conserved (Fig. 2). Based on these analyses, we conclude that *Pf*RON3 (PFL2505c) is an authentic ortholog of *Tg*RON3 (TGME49_023920).

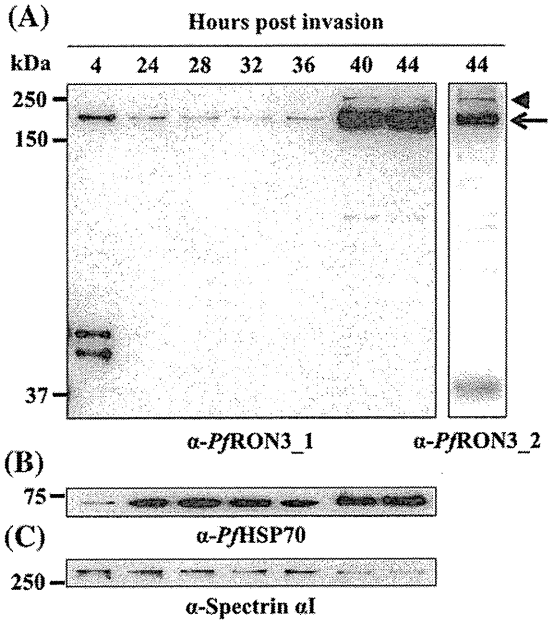

Fig. 3. Stage-specific expression profile of *Pf*RON3. Proteins from synchronized parasite cultures were harvested at each time point and separated by SDS-PAGE on a 12.5% gel under reducing condition. (A) Using either anti-*Pf*RON3_1- or anti-*Pf*RON3_2- specific antibodies, a band of approximately 260 kDa (arrowhead) was detected in late stages (40–44 h post invasion) and a 190-kDa band (arrow) was detected in both the schizont, ring, and trophozoite stage parasites. (B and C) Loading controls. To ensure that equal amounts of the stage-specific samples were loaded in each lane for western blot analysis, the membranes were probed with anti-*Pf*HSP70 monoclonal antibody (4C9) as a quantitative parasite protein marker [36], and anti-human spectrin α I rabbit antibody indicating the number of erythrocytes. The intensity of the *Pf*HSP70 bands indicated that the amount of sample loaded in each lane was comparable.

T. gondii RON3 protein was originally suggested to be localized at the rhoptry neck by immunofluorescence assay [12]. In contrast, our current immunoelectron microscopy results confirmed that *Pf*RON3 localizes in the rhoptry body rather than the rhoptry neck. Since *Pf*RON3 is in the rhoptry body, we are tempted to think that TgRON3 is also localizes in the rhoptry body rather than the rhoptry neck. Therefore we believe that the localization of *Tg*RON3 should be reconfirmed by electron microscopy using quality antibodies. In general, the biggest technical hurdle to obtaining antibodies of adequate quality for use in electron microscopy studies of this sort would be the ability to produce correctly folded recombinant proteins in sufficient quantity and purity [31]. The immunoelectron microscopy results we obtained clearly demonstrate that high quality antibodies can be successfully produced using quality proteins synthesized in the wheat germ cell-free protein production system. We have already [14–16] demonstrated that the wheat germ cell-free protein production system enables the expression of quality recombinant proteins without codon optimization.

In our stage-specific western blot and immunofluorescence microscopy analyses for the *Pf*RON3 expression profile, we detected *Pf*RON3 not only in the merozoite rhoptry body but also in the PV of ring stage parasites (Fig. 6). Previous studies showed that well-characterized rhoptry body proteins (*Pf*RhopH complex, *Pf*RAP complex, and *Pf*RAMA) are discharged into the PV [32–34]. Therefore, the secretory pathway of *Pf*RON3 into the PV might be similar to that of these rhoptry body proteins. Additionally, since the 260-kDa band, corresponding to full-length *Pf*RON3, is only visible at the schizont stage (40–44 h post invasion) (Fig. 3A), the processed 190-kDa fragment may contain the functional domains throughout the parasite's asexual erythrocytic cycle.

Finally, our immunoprecipitation studies demonstrated that *Pf*RON2, *Pf*RON3, and *Pf*RON4, are able to interact and form a novel complex *in vitro*, even in the absence of *Pf*AMA1, indicating that the formation of this novel RON complex is independent of *Pf*AMA1. These results are in agreement with the previously published results showing that *Pf*RON2 and *Pf*RON4 are able to interact and form a complex independently, in the absence of *Pf*AMA1 and in the parasite; most AMA1 is not associated with complexes that contain *Pf*RON2 and *Pf*RON4 [35]. However, in this study we were unable to confirme the

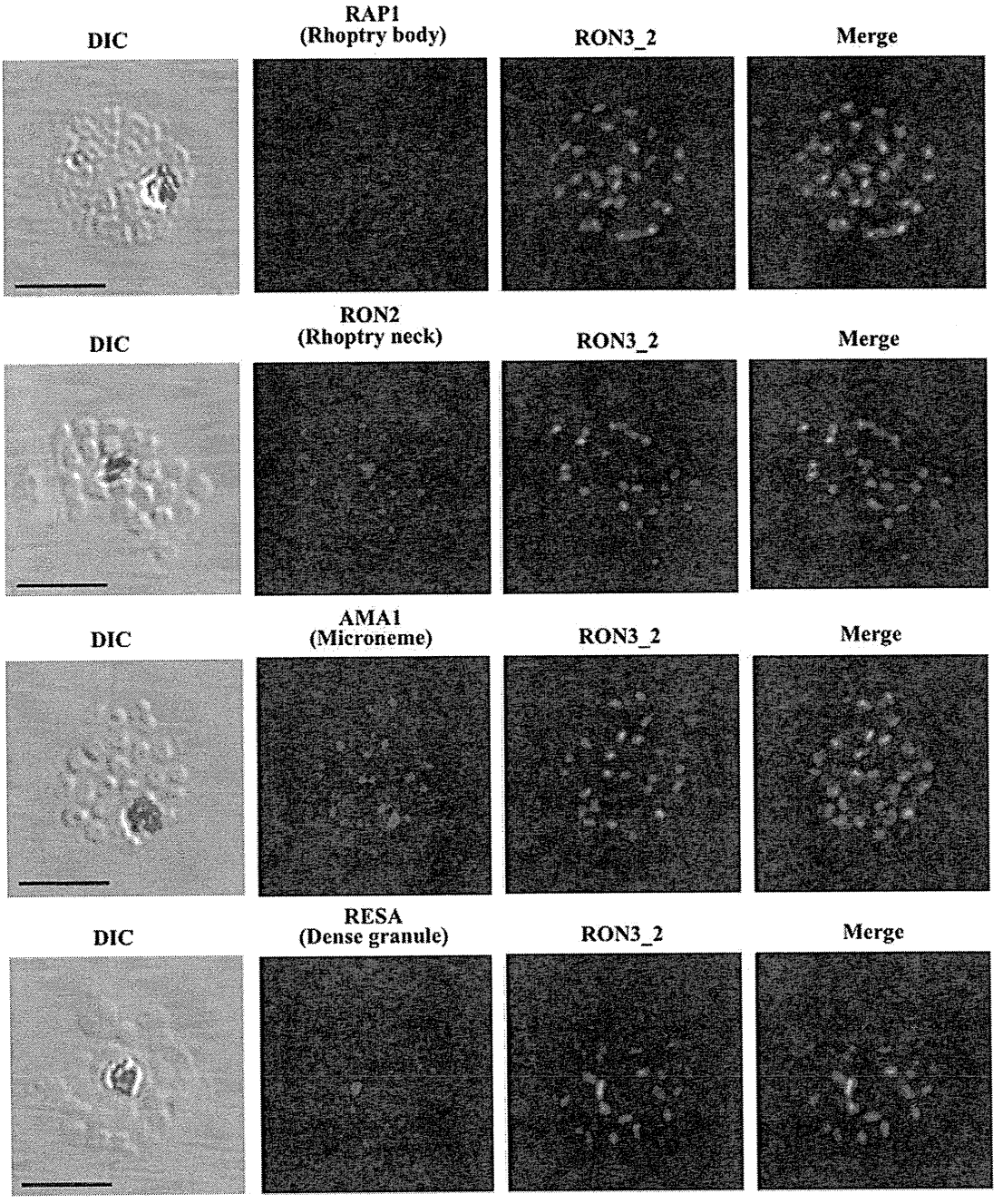

Fig. 4. *Pf*RON3 is expressed at the apical end of *Plasmodium* merozoites. Schizont and merozoite stage parasites were dual-labeled with antisera against *Pf*RON3_2 and either *Pf*RAP1 (rhoptry body marker), *Pf*RON2 (rhoptry neck marker), *Pf*AMA1 (microneme marker), or *Pf*RESA (dense granule marker). Nuclei are visualized with DAPI in merged images shown in the right panels. Bars represent 5 μm.

localization of *Pf*RON3 and the timing of the novel complex formation during the merozoite invasion process. Hence, the role of *Pf*RON3 and the novel complex in formation of the moving junction and the merozoite invasion process could not be elucidated. It will be interesting to undertake further experiments to shed light on the localization and function of *Pf*RON3 and the novel complex during merozoite invasion.

In summary, our results show that *Pf*RON3 is a rhoptry body protein, not a rhoptry neck protein, and that it interacts with *Pf*RON2 and *Pf*RON4, but not with *Pf*AMA1. These results suggest that *Pf*RON3 partakes in the novel *Pf*RON complex formation (*Pf*RON2, 3, and 4), but not in formation of the moving junction complex (*Pf*RON2, 4, 5, and *Pf*AMA1). The novel *Pf*RON complex, as well as the moving junction complex, might play a fundamental role in erythrocyte invasion by merozoite stage parasites.

Acknowledgments

We are grateful to Jean F. Dubremetz for providing the anti-*Pf*RON4 monoclonal antibody, Robin F. Anders for providing the anti-*Pf*RESA monoclonal antibody, and Niwat Kangwanrangsan for providing the mouse anti-*Pf*EXP2 antibody. We thank Masachika Shudo and Keizou Oka, Integrated Center for Science, Ehime University, Japan for technical assistance. We thank Thangavelu U. Arumugam for critical

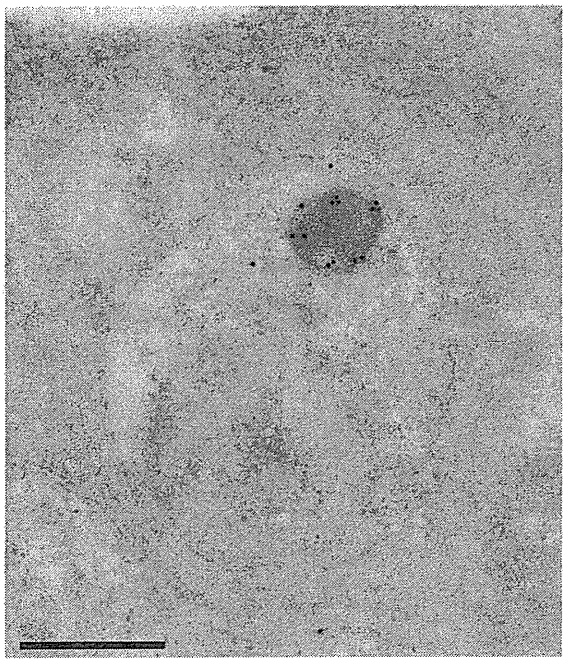

Fig. 5. Rhoptry body localization of *Pf*RON3 by immunoelectron microscopy. Longitudinally sectioned merozoites in mature schizonts were labeled with rabbit anti-*Pf*RON3_2 antibodies followed by secondary antibody conjugated with gold particles. The image shows that the gold particle signals were restricted to the merozoite rhoptry body. Bar represents 500 nm.

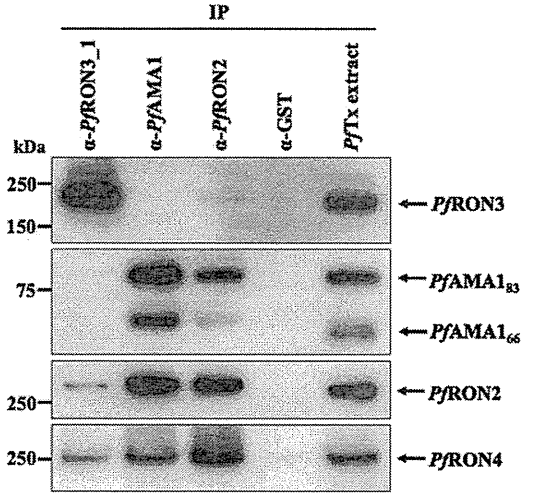

Fig. 7. *Pf*RON3 is not involved in the RON–AMA1 complex. Triton X-100 extracts of schizont-rich parasite (*Pf*Tx extract) were immunoprecipitated (IP) with rabbit sera against *Pf*RON3 (α-*Pf*RON3_1), *Pf*AMA1 (α-*Pf*AMA1), *Pf*RON2 (α-*Pf*RON2), or GST (α-GST), then stained with mouse antisera against *Pf*RON3, *Pf*AMA1, *Pf*RON2, or *Pf*RON4, respectively. Immunoprecipitation using anti-GST antibody was used as a negative control. No bands were detected in the anti-GST immunoprecipitate, indicating the exclusion of potential carryover of proteins due to insufficient or inadequate washing steps.

reading of the manuscript. This research was supported by the Ministry of Education, Culture, Sports, Science and Technology (21249028 and 21022034), and by the Ministry of Health, Labour,

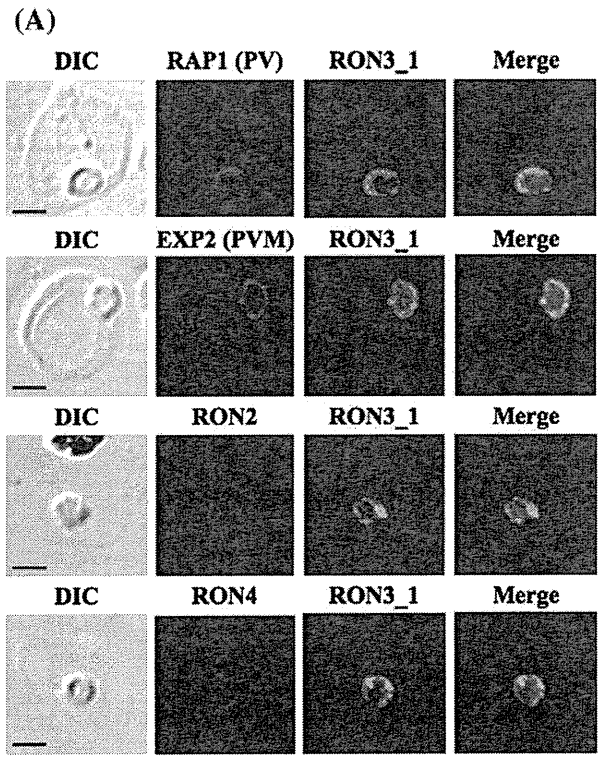

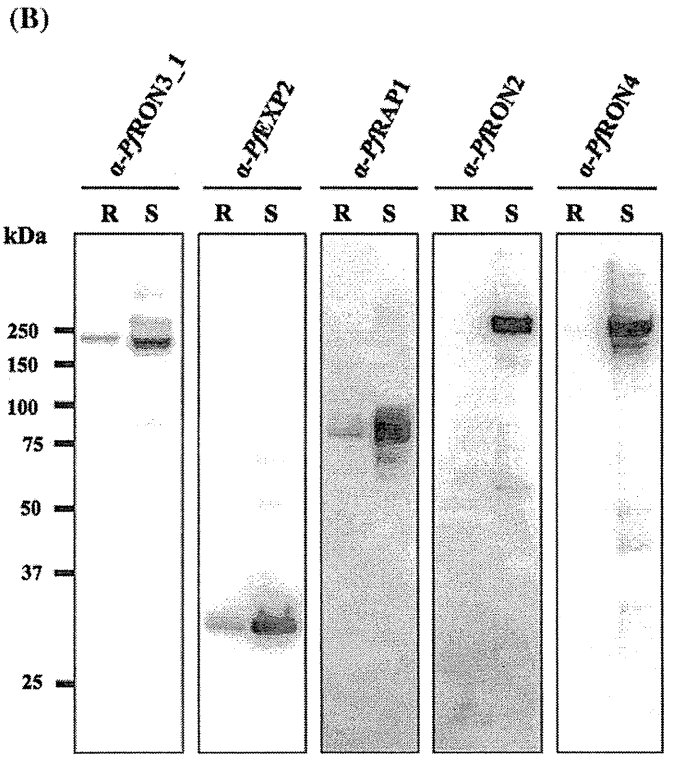

Fig. 6. *Pf*RON3 is found in the parasitophorous vacuole in ring stage parasites. (A) Ring stage parasites were dual-labeled with antisera against *Pf*RON3_1 and either *Pf*RAP1 (PV marker), *Pf*EXP2 (PVM marker), *Pf*RON2, or *Pf*RON4. Nuclei are visualized with DAPI in merged images shown in the right panels. Bars represent 2.5 μm. (B) Proteins from synchronized parasite cultures were harvested at the ring stage (R) and schizont stage (S), and separated by SDS-PAGE on a 12.5% gel under a reducing condition. After transfer of proteins onto a PVDF membrane, the membrane was stained using rabbit anti-*Pf*RON3_1, mouse anti-*Pf*RAP1, anti-*Pf*EXP2, anti-*Pf*RON2, anti-*Pf*RON4 antibodies.

and Welfare, Japan (H20-Shinkou-ippan-013 and H21-Chikyukibo-ippan-005).

Appendix A. Supplementary data

Supplementary data to this article can be found online at doi:10.1016/j.parint.2011.01.001.

References

[1] Hay SI, Guerra CA, Gething PW, Patil AP, Tatem AJ, Noor AM, et al. A world malaria map: *Plasmodium falciparum* endemicity in 2007. PLoS Med 2009;6:e1000048.
[2] Cowman AF, Crabb BS. Invasion of red blood cells by malaria parasites. Cell 2006;124:755–66.
[3] Kaneko O. Erythrocyte invasion: vocabulary and grammar of the *Plasmodium* rhoptry. Parasitol Int 2007;56:255–62.
[4] Aikawa M, Miller LH, Johnson J, Rabbege J. Erythrocyte entry by malarial parasites. A moving junction between erythrocyte and parasite. J Cell Biol 1978;77:72–82.
[5] Lebrun M, Michelin A, El Hajj H, Poncet J, Bradley PJ, Vial H, et al. The rhoptry neck protein RON4 re-localizes at the moving junction during *Toxoplasma gondii* invasion. Cell Microbiol 2005;7:1823–33.
[6] Alexander DL, Mital J, Ward GE, Bradley P, Boothroyd JC. Identification of the moving junction complex of *Toxoplasma gondii*: a collaboration between distinct secretory organelles. PLoS Pathog 2005;1:e17.
[7] Alexander DL, Arastu-Kapur S, Dubremetz JF, Boothroyd JC. *Plasmodium falciparum* AMA1 binds a rhoptry neck protein homologous to *Tg*RON4, a component of the moving junction in *Toxoplasma gondii*. Eukaryot Cell 2006;5:1169–73.
[8] Cao J, Kaneko O, Thongkukiatkul A, Tachibana M, Otsuki H, Gao Q, et al. Rhoptry neck protein RON2 forms a complex with microneme protein AMA1 in *Plasmodium falciparum* merozoites. Parasitol Int 2009;58:29–35.
[9] Richard D, MacRaild CA, Riglar DT, Chan JA, Foley M, Baum J, et al. Interaction between *Plasmodium falciparum* apical membrane antigen 1 and the rhoptry neck protein complex defines a key step in the erythrocyte invasion process of malaria parasites. J Biol Chem 2010;285:14815–22.
[10] Triglia T, Healer J, Caruana SR, Hodder AN, Anders RF, Crabb BS, et al. Apical membrane antigen 1 plays a central role in erythrocyte invasion by *Plasmodium* species. Mol Microbiol 2000;38:706–18.
[11] Hehl AB, Lekutis C, Grigg ME, Bradley PJ, Dubremetz JF, Ortega-Barria E, et al. *Toxoplasma gondii* homologue of *Plasmodium* apical membrane antigen 1 is involved in invasion of host cells. Infect Immun 2000;68:7078–86.
[12] Bradley PJ, Ward C, Cheng SJ, Alexander DL, Coller S, Coombs GH, et al. Proteomic analysis of rhoptry organelles reveals many novel constituents for host–parasite interactions in *Toxoplasma gondii*. J Biol Chem 2005;280:34245–58.
[13] Trager W, Jensen JB. Human malaria parasites in continuous culture. Science 1976;193:673–5.
[14] Tsuboi T, Takeo S, Iriko H, Jin L, Tsuchimochi M, Matsuda S, et al. Wheat germ cell-free system-based production of malaria proteins for discovery of novel vaccine candidates. Infect Immun 2008;76:1702–8.
[15] Tsuboi T, Takeo S, Sawasaki T, Torii M, Endo Y. An efficient approach to the production of vaccines against the malaria parasite. Meth Mol Biol 2010;607: 73–83.
[16] Tsuboi T, Takeo S, Arumugam TU, Otsuki H, Torii M. The wheat germ cell-free protein synthesis system: a key tool for novel malaria vaccine candidate discovery. Acta Trop 2010;114:171–6.
[17] Culvenor JG, Day KP, Anders RF. *Plasmodium falciparum* ring-infected erythrocyte surface antigen is released from merozoite dense granules after erythrocyte invasion. Infect Immun 1991;59:1183–7.
[18] Hiller NL, Akompong T, Morrow JS, Holder AA, Haldar K. Identification of a stomatin orthologue in vacuoles induced in human erythrocytes by malaria parasites. A role for microbial raft proteins in apicomplexan vacuole biogenesis. J Biol Chem 2003;278:48413–21.
[19] Kaneko O, Fidock DA, Schwartz OM, Miller LH. Disruption of the C-terminal region of EBA-175 in the Dd2/Nm clone of *Plasmodium falciparum* does not affect erythrocyte invasion. Mol Biochem Parasitol 2000;110:135–46.
[20] Torii M, Adams JH, Miller LH, Aikawa M. Release of merozoite dense granules during erythrocyte invasion by *Plasmodium knowlesi*. Infect Immun 1989;57: 3230–3.
[21] Aikawa M, Atkinson CT. Immunoelectron microscopy of parasites. Adv Parasitol 1990;29:151–214.
[22] Altschul SF, Madden TL, Schaffer AA, Zhang J, Zhang Z, Miller W, et al. Gapped BLAST and PSI-BLAST: a new generation of protein database search programs. Nucleic Acids Res 1997;25:3389–402.
[23] Bahl A, Brunk B, Crabtree J, Fraunholz MJ, Gajria B, Grant GR, et al. PlasmoDB: the *Plasmodium* genome resource. A database integrating experimental and computational data. Nucleic Acids Res 2003;31:212–5.
[24] Bendtsen JD, Nielsen H, von Heijne G, Brunak S. Improved prediction of signal peptides: SignalP 3.0. J Mol Biol 2004;340:783–95.
[25] Krogh A, Larsson B, von Heijne G, Sonnhammer EL. Predicting transmembrane protein topology with a hidden Markov model: application to complete genomes. J Mol Biol 2001;305:567–80.
[26] Schultz J, Milpetz F, Bork P, Ponting CP. SMART, a simple modular architecture research tool: identification of signaling domains. Proc Natl Acad Sci USA 1998;95: 5857–64.
[27] Thompson JD, Higgins DG, Gibson TJ. CLUSTAL W: improving the sensitivity of progressive multiple sequence alignment through sequence weighting, position-specific gap penalties and weight matrix choice. Nucleic Acids Res 1994;22:4673–80.
[28] Baldi DL, Andrews KT, Waller RF, Roos DS, Howard RF, Crabb BS, et al. RAP1 controls rhoptry targeting of RAP2 in the malaria parasite *Plasmodium falciparum*. EMBO J 2000;19:2435–43.
[29] Johnson D, Gunther K, Ansorge I, Benting J, Kent A, Bannister L, et al. Characterization of membrane proteins exported from *Plasmodium falciparum* into the host erythrocyte. Parasitology 1994;109(Pt 1):1–9.
[30] Fischer K, Marti T, Rick B, Johnson D, Benting J, Baumeister S, et al. Characterization and cloning of the gene encoding the vacuolar membrane protein EXP-2 from *Plasmodium falciparum*. Mol Biochem Parasitol 1998;92:47–57.
[31] Proellocks NI, Coppel RL, Waller KL. Dissecting the apicomplexan rhoptry neck proteins. Trends Parasitol 2010;26:297–304.
[32] Sam-Yellowe TY, Shio H, Perkins ME. Secretion of *Plasmodium falciparum* rhoptry protein into the plasma membrane of host erythrocytes. J Cell Biol 1988;106: 1507–13.
[33] Howard RF, Stanley HA, Campbell GH, Reese RT. Proteins responsible for a punctate fluorescence pattern in *Plasmodium falciparum* merozoites. Am J Trop Med Hyg 1984;33:1055–9.
[34] Topolska AE, Lidgett A, Truman D, Fujioka H, Coppel RL. Characterization of a membrane-associated rhoptry protein of *Plasmodium falciparum*. J Biol Chem 2004;279:4648–56.
[35] Collins CR, Withers-Martinez C, Hackett F, Blackman MJ. An inhibitory antibody blocks interactions between components of the malarial invasion machinery. PLoS Pathog 2009;5:e1000273.
[36] Tsuji M, Mattei D, Nussenzweig RS, Eichinger D, Zavala F. Demonstration of heat-shock protein 70 in the sporozoite stage of malaria parasites. Parasitol Res 1994;80:16–21.

Parasitol Res
DOI 10.1007/s00436-011-2370-z

ORIGINAL PAPER

Measurement of naturally acquired humoral immune responses against the C-terminal region of the *Plasmodium vivax* MSP1 protein using protein arrays

Jun-Hu Chen · Yue Wang · Kwon-Soo Ha · Feng Lu · In-Bum Suh · Chae Seung Lim · Jeong Hyun Park · Satoru Takeo · Takafumi Tsuboi · Eun-Taek Han

Received: 10 January 2011 / Accepted: 25 March 2011

Abstract Protein arrays are powerful tools for antibody profiling and vaccine development against infectious agents. In the previous report, we successfully applied an antibody-based protein array for immunoprofiling of *Plasmodium vivax* infection. Herein, we developed a Ni-NTA surface based protein array to detect immune responses against the recombinant C-terminal region (19 and 42 kDa) of the *P. vivax* merozoite surface protein 1 (PvMSP1-19 and -42) from sera of vivax malaria patients. The PvMSP1-19 arrays detected *P. vivax* in 112 of 130 (86.2%; 95% CI, 83.2–89.2%) microscopically positive samples and 2 false positives were obtained among 100 sera samples from healthy subjects (2.0%; 95% CI, 0.6–3.4%). These results were in concordance with results of enzyme-linked immunosorbent assays (ELISA). Kappa values represented excellent agreement for the recombinant PvMSP1-19 protein against sera samples as measured by protein arrays and ELISA (Kappa=0.904, 95% CI:

J.-H. Chen and Y. Wang contributed equally to this work.

E.-T. Han and T. Tsuboi are co-corresponding author.

J.-H. Chen · Y. Wang · F. Lu · E.-T. Han (✉)
Department of Parasitology and Institute of Medical Science,
Kangwon National University School of Medicine,
Hyoja2-dong,
Chunchon 200-701, Kangwon-do,
Republic of Korea
e-mail: ethan@kangwon.ac.kr

J.-H. Chen · Y. Wang
Institute of Parasitic Diseases,
Zhejiang Academy of Medical Sciences,
Hangzhou 310013, People's Republic of China

J.-H. Chen
National Institute of Parasitic Diseases,
Chinese Center for Disease Control and Prevention,
Shanghai 20025, People's Republic of China

K.-S. Ha
Department of Molecular and Cellular Biochemistry
and Institute of Medical Science,
Kangwon National University School of Medicine,
Chunchon 200-701, Republic of Korea

F. Lu
Jiangsu Institute of Parasitic Diseases,
Wuxi 214064, People's Republic of China

I.-B. Suh
Department of Laboratory Medicine
and Institute of Medical Science,
Kangwon National University School of Medicine,
Chunchon 200-701, Republic of Korea

C. S. Lim
Department of Laboratory Medicine, College of Medicine,
Korea University,
Seoul, Republic of Korea

J. H. Park
Department of Anatomy and Cell Biology,
Kangwon National University School of Medicine,
Chunchon 200-701, Republic of Korea

S. Takeo · T. Tsuboi (✉)
Cell-Free Science and Technology Research Center,
Ehime University,
Matsuyama, Ehime 790-8577, Japan
e-mail: tsuboi@ccr.ehime-u.ac.jp

Published online: 13 April 2011

0.849–0.960). The PvMSP1-42 protein arrays detected antibody response in 100 of 130 microscopically positive samples (76.9%; 95% CI, 72.4–86.8%) and 8 false positives were obtained in 100 healthy subjects (8.0%; 95% CI, 2.7–13.3%). There is no significant difference between the fluorescent intensity of antibody response to PvMSP1-19 and PvMSP1-42 in the positive sera samples ($P>0.05$). The novel protein array platform may be used for profiling naturally acquired humoral immune responses to *P. vivax* infection.

Introduction

Among the malaria parasites that infect humans, *Plasmodium vivax* threatens almost 40% of the world's population, resulting in 132–391 million clinical infections each year (Price et al. 2007). In South and Southeast Asia, where the majority of vivax malaria infections occur, *P. vivax* accounts for up to 50% of malaria cases, with prevalence rates between 1% and 6% of the population. The emergence of chloroquine-resistant *Plasmodium falciparum* has reduced the proportion of malaria cases due to *P. vivax*; nevertheless, the absolute numbers of *P. vivax* remain high (Price et al. 2007; Mueller et al. 2009).

During the erythrocytic stages of malaria infection, potential targets for an immune response are free merozoites or intraerythrocytic parasites, and it is assumed that humoral antibody responses play a major role in blood-stage immunity (Langhorne et al. 2008). The mechanisms by which antibodies are effective include blockage of red blood cell (RBC) invasion by merozoites, antibody-dependent cellular killing mediated by cytophilic antibodies, and binding of antibodies to parasite-induced molecules on the RBC surface, thus leading to greater clearance of infected RBCs (Richie and Saul 2002). Antibodies are typically measured using an enzyme-linked immunosorbent assay (ELISA), a technique that requires high amounts of coating-antigens and immune sera when large numbers of samples must be screed (Fernandez-Becerra et al. 2010). To overcome these limitations, protein arrays with high-throughput capacity to detect specific antibody responses with minimal amounts of immune sera have been developed (Parekh and Richie 2007). This methodology has already been shown to be useful in the serodiagnosis and vaccine development of infectious diseases (Mezzasoma et al. 2002; Davies et al. 2005; Zhu et al. 2006; Felgner et al. 2009).

P. vivax merozoite surface protein 1 (PvMSP1) is a glycosylphosphatidylinositol (GPI)-anchored membrane protein expressed abundantly on the merozoite surface. Several studies have demonstrated the high antigenicity of the C-terminal region (19 or 42 kDa) of PvMSP1 (PvMSP1-19 and -42) worldwide, including countries such as Brazil, India, Sri Lanka, and Turkey (Cunha et al. 2001; Sachdeva et al. 2004; Wickramarachchi et al. 2007; Zeyrek et al. 2008). Protective efficacy has been observed in preclinical vaccine trials using *P. falciparum* recombinant C-terminal regions of MSP1 (PfMSP1-19), which has stimulated the study of *P. vivax* recombinant MSP1-19 (Collins et al. 1999). Partial protection *P. vivax* C-terminal region was observed in the first trial, and effective protection was achieved in the second trial (Perera et al. 1998).

In the present study, recombinant PvMSP1-19 and -42 were expressed using a wheat germ cell-free expression (WGCE) system. This technology is known to be a suitable system for decoding malaria genes without any codon optimization into biologically active malaria proteins (Tsuboi et al. 2008; Chen et al. 2010a). PvMSP1-19 and -42 were used to profile naturally acquired humoral immune responses in human patients infected with *P. vivax* in the Republic of Korea, and the protein array technology was validated.

Materials and methods

Patient samples

A total of 130 blood samples were obtained from patients who were confirmed positive for vivax malaria via microscopy at Korea University Ansan Hospital and at local health centers and clinics in Gyeonggi and Gangwon Provinces within endemic areas of the Republic of Korea. A total of 100 blood samples were taken from healthy patients who were confirmed negative for vivax malaria by microscopy, and these were used as controls. This study was approved by the Institutional Review Board at Kangwon National University Hospital.

Cloning of the gene encoding PvMSP1-19 and -42

The gene fragment encoding PvMSP1-19 was amplified by PCR from genomic DNA of the *P. vivax* Sal I strain, and cloned into the pEU-E01-His-Tev-N2 vector (CellFree Sciences, Matsuyama, Japan) at the *Xho* I and *Not* I sites. The inserted nucleotide sequence was confirmed using the ABI PRISM 310 Genetic Analyzer and a BigDye Terminator v1.1 Cycle Sequencing kit (Applied Biosystems, Foster City, CA, USA). The gene fragment encoding PvMSP1-42 was amplified by PCR from genomic DNA of the *P. vivax* isolate from Republic of Korea, and cloned into the pEU-E01-His-Tev-N2 vector by In-Fusion cloning method (Chen et al. 2010a). Highly purified plasmid DNA is required for in vitro transcription and subsequent translation. Plasmid DNA was then prepared using the Maxi Plus™ Ultrapure plasmid extraction system (Viogene,

Taipei, Taiwan) according to the manufacturer's instructions. Purified DNA was eluted in 0.1×TE buffer (10 mM Tris–HCl, pH 8.0, 1 mM EDTA) and used for recombinant protein expression by WGCE.

Production of recombinant PvMSP1-19 and -42 using a wheat germ cell-free expression system

P. vivax MSP1-19 was expressed by 12 wells in a 6-well plate scale of the WGCE system using previously described bilayer translation reaction methods (Tsuboi et al. 2008; Chen et al. 2010a). The recombinant PvMSP1-19 protein was purified using a Ni-nitrilotriacetic acid agarose column (Qiagen, Valencia, CA, USA). PvMSP1-42 was expressed by a 1 ml WGCE system using the bilayer translation reaction method (Chen et al. 2010a). A WEPRO®1240H kit (CellFree Sciences) was used to synthesize PvMSP1-19 and -42.

SDS-PAGE and Western blot analysis

The recombinant PvMSP1-19 and -42 proteins were separated by SDS-PAGE under reducing conditions. The separated proteins were transferred to 0.45 μm PVDF membranes (Millipore, Billerica, MA, USA) in a semi-dry transfer buffer (50 mM Tris, 190 mM glycine, 3.5 mM SDS, 20% methanol) at a constant 400 mA for 40 min using a semi-dry blotting system (ATTO Corp., Tokyo, Japan). After blocking with 5% skim milk in TBS/T, penta-His antibody (Qiagen, Valencia, CA, USA) and secondary alkaline phosphatase-conjugated goat anti-mouse IgG (ICN-Cappel, Costa Mesa, CA, USA) were used to detect His-tagged recombinant proteins. The immunoblots were incubated with a BCIP/NBT color development solution.

ELISA

To validate the immunoreactivity detected by protein arrays, sera from 130 vivax malaria patients in endemic areas of the Republic of Korea and 100 healthy individuals were tested against recombinant PvMSP1-19 protein by ELISA, as described previously (Mehrizi et al. 2009). The positive cut-off value was calculated as the mean optical density (OD) of normal controls plus 2 standard deviations (SD). Sera were screened by protein arrays as described below.

Serum screening using protein arrays

Sera from 130 vivax malaria patients and 100 healthy individuals were tested against the recombinant PvMSP1-19 protein using protein arrays. One microliter of recombinant PvMSP1-19 protein (40 ng/μl) or crude PvMSP1-42 protein was spotted to each well of a Ni^{2+} chelated (Xenopore Corp., Hawthorne, NJ, USA) surface slide and incubated for 2 h at 37°C. The arrays were first blocked with 5% BSA in PBS-T for 1 h at 37°C. Then they were probed with human serum (1:200) that was first pre-absorbed against wheat germ lysate (1:100) to block anti-wheat germ antibodies. The arrays were incubated with serum in PBS-T for 1 h at 37°C and antibodies were visualized with 10 ng/μl Alexa Fluor 546 goat anti-human IgG (Invitrogen, Carlsbad, CA, USA) in PBS-T and scanned in a fluorescence scanner (ScanArray Express, PerkinElmer, Boston, MA, USA) (Park et al. 2009). Fluorescence intensities of array spots were quantified by the fixed circle method using ScanArray Express software (version 4.0, PerkinElmer). The positive cut-off value was calculated as the mean fluorescence intensity (MFI) value of the negative controls plus 2 SD.

Statistical analyses

Ninety-five percent confidence intervals (95% CI) were calculated according to a previous report (Chen et al. 2010b). The correlation between duplicate spots of protein arrays and the antibody reactivity of different recombinant PvMSP1 protein concentrations were analyzed using the Origin program (version 6.1, OriginLab). OD and MFI values from different samples were plotted using GraphPad Software version 5.0 (GraphPad Software, San Diego, CA, USA). Concordance in seropositivity responses between the two methods was evaluated using Kappa statistics. According to a previous report, excellent agreement was defined as a Kappa value>0.9 (Fernandez-Becerra et al. 2010).

Results

SDS-PAGE analysis showed that the band of purified recombinant PvMSP1-19 protein appeared at about 14 kDa, which is similar to the predicted size of PvMSP1-19 plus the amino acids of the multiple cloning site (MCS) remaining on the plasmid vector (Fig. 1a). Western blot analysis showed one specific band of PvMSP1-19 at 14 kDa (Fig. 1b). These results indicate that the PvMSP1-19 was successfully expressed by WGCE and purified. The result of western blot analysis of PvMSP1-42 was described previously (Chen et al. 2010a).

The efficiency of protein arrays for antibody profiling was evaluated using purified PvMSP1-19 (Fig. 2a, right panel). A novel concentration-dependent analysis method showed a correlation coefficient of 0.98 between fluorescence intensities and protein concentrations (Fig. 2b). Because a high concentration of protein coating may lead to saturation of the antigen-antibody reaction, we determined the appropriate concentration (40 ng/μl) of protein coating for Ni^{2+}-chelated slides. One protein array probed

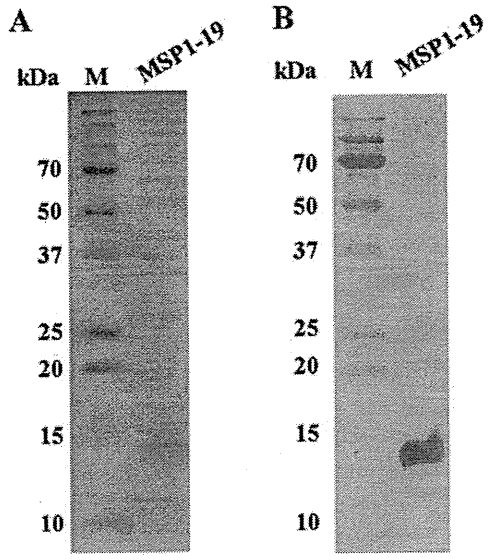

Fig. 1 SDS-PAGE and Western blot analysis of recombinant PvMSP1-19. **a** Recombinant PvMSP1-19 protein was stained with Coomassie brilliant blue. **b** Recombinant PvMSP1-19 protein was detected by anti-His antibody. M, protein marker

with serum from healthy individuals and vivax malaria patients is shown in the left panel of Fig. 2a. Sera from malaria-naive subjects showed low reactivity, whereas that from *P. vivax*-exposed individuals showed obvious reactivity against PvMSP1-19 (Fig. 2a, left panel). When relative intensities of duplicate spots were plotted against each other, the resulting diagonal indicated a good reproducibility of spotting and detection of the immobilized proteins with a correlation coefficient of 0.98 (Fig. 2c).

Antibody responses against recombinant PvMSP1-19 in sera samples from 130 patients infected with *P. vivax* and 100 healthy individuals were detected using ELISA and protein arrays. Both methods showed apparent differences between the two groups of samples (Fig. 3a, b). The average OD value of samples from infected patients ($OD_{450\ nm}$=1.625) was significantly higher than that of healthy individuals ($OD_{450\ nm}$=0.132). In the same manner, the average fluorescent intensity value of sera samples from infected patients (fluorescent intensity=27,572 a.u.) was significantly higher than that of healthy individuals (fluorescent intensity=1,933 a.u.) (Table 1).

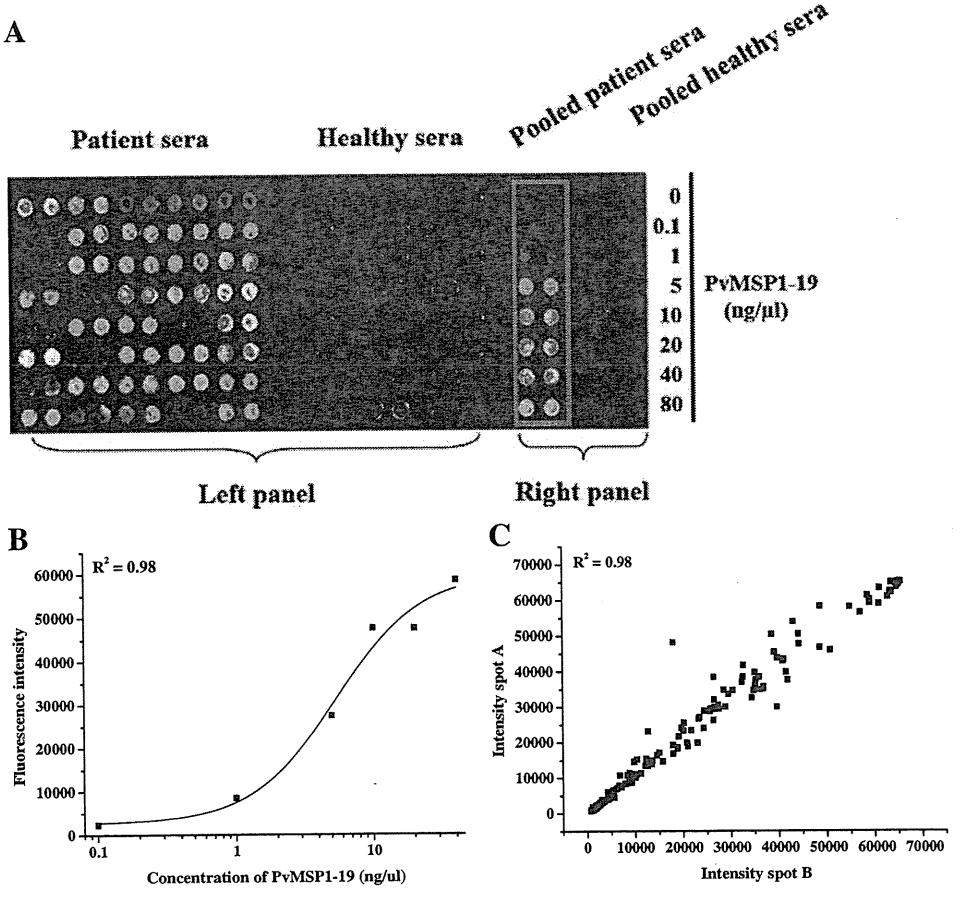

Fig. 2 Development of a protein array platform for profiling antibody responses to *P. vivax* infection. **a** *Left panel* Recombinant PvMSP1-19 (40 ng/μl) reacted with individual serum samples. *Right panel* Different concentrations of recombinant PvMSP1-19 protein were probed with pooled human serum (left duplicate, positive serum; right duplicate, negative serum). **b** Correlation between spot intensities and the concentration of recombinant PvMSP1-19. **c** Correlation between relative spot intensities of duplicates (*spot a* versus its duplicate *spot b*)

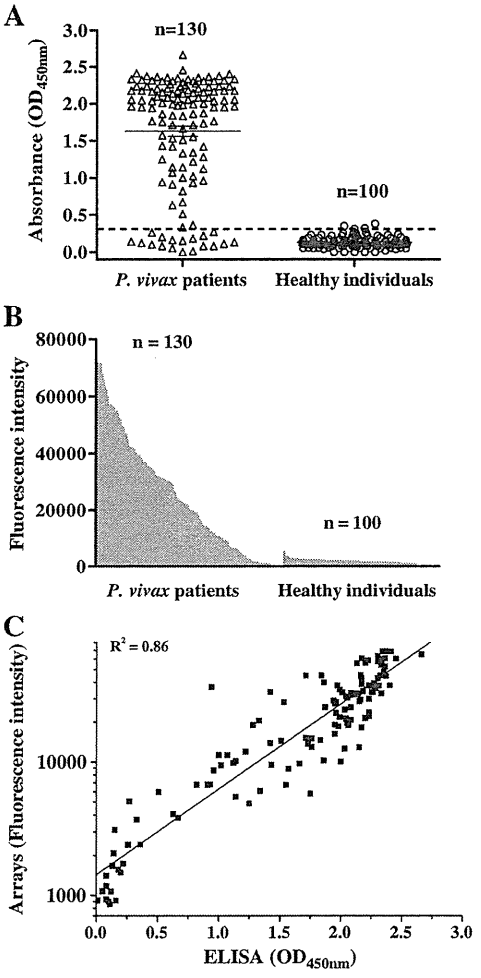

Fig. 3 IgG antibody responses to recombinant PvMSP1-19 protein using ELISA and protein arrays. Sera samples from *P. vivax*-infected patients (n=130) and healthy individuals (n=100) were measured by ELISA (**a**) and protein arrays (**b**). **c** Correlation between ELISA and protein arrays for antibody profiling

Both the ELISA and the protein arrays detected *P. vivax* in 112 of 130 of the microscopically confirmed positive samples (86.2%; 95% CI, 83.2–89.2%) (Table 2). Out of the 100 sera samples from healthy subjects, five false positives were obtained by ELISA (5.0%; 95% CI, 2.8–7.2%), whereas two false positives were obtained by protein arrays (2.0%; 95% CI, 0.6–3.4%) (Table 2). The Kappa values represented excellent agreement for recombinant PvMSP1-19 proteins against sera samples measured by ELISA and protein arrays (Kappa=0.904, 95% CI: 0.849–0.960 and total agreement=95.2%).

The ELISA absorbance readings for antibody response against PvMSP1-19 in sera samples from *P. vivax*-infected patients were compared to the fluorescence measurements obtained by protein arrays. The ELISA and array data correlated well, with a correlation coefficient of 0.86 (Fig. 3c).

To test the efficiency of antibody response against crude *P. vivax* protein using Ni^{2+}-chelated surface slides, crude His-tagged PvMSP1-42 was used for in situ binding and purification. One protein array probed with serum from healthy individuals and vivax malaria patients is shown in Fig. 4a. Sera from malaria-naive subjects showed low reactivity, whereas those from *P. vivax*-exposed individuals showed obvious reactivity against PvMSP1-42 (Fig. 4a). When relative intensities of duplicate spots were plotted against each other, the resulting diagonal indicated a good reproducibility of spotting and detection of the immobilized proteins with a correlation coefficient of 0.98 (Fig. 4b). Protein arrays detected *P. vivax* in 100 of 130 sera samples from the microscopically positive samples (76.9%; 95% CI, 72.4–86.8%). From the 100 sera samples from healthy subjects, eight false positives were obtained by protein arrays (8.0%; 95% CI, 2.7–13.3%). There is no significant difference between the fluorescent intensity of antibody response to purified PvMSP1-19 and crude PvMSP1-42 in the positive sera samples (P>0.05).

Discussion

New methods for rapid gene cloning, and high-throughput cell-free protein expression are now publicly available in post-genomic malaria research (Gardner et al. 2002; Aguiar et al. 2004; Tsuboi et al. 2008). These methods promote the development of high-throughput assays for profiling immune responses against infectious diseases. Some work has focused on the development of subproteome or proteome arrays for smaller pathogens to identify immunodominant

Table 1 Analysis of optical density (OD) values and mean fluorescence intensities (MFI) of IgG antibodies against PvMSP1-19 in sera samples using ELISA and protein arrays, respectively

Source of human serum samples	Total no. of samples	Screening methods for antibody profiling			
		ELISA ($OD_{450\ nm}$)		Protein arrays (MFI)	
		Mean	SD	Mean	SD
Vivax malaria patients	130	1.625	0.770	27,572	22,406
Healthy individuals	100	0.132	0.077	1,933	789

Table 2 Frequency distribution of IgG antibodies against PvMSP1-19 in sera samples using ELISA and protein arrays, respectively

Source of human serum samples	Total no. of sample	Screening methods for antibody profiling			
		ELISA		Protein arrays	
		No. positive	Frequency (%) (95% CI)	No. positive	Frequency (%) (95% CI)
Malaria patients	130	112	86.2 (83.2–89.2)	112	86.2 (83.2–89.2)
Healthy individuals	100	5	5.0 (2.8–7.2)	2	2.0 (0.6–3.4)

Kappa values presented good agreement for the recombinant PvMSP1-19 protein against sera samples measured by ELISA and protein arrays (Kappa=0.904 and total agreement=95.2%)

antigens (Steller et al. 2005; Davies et al. 2007; Beare et al. 2008; Davies et al. 2008). The results verify this platform as a rapid way to comprehensively scan humoral immunity of vaccinated or infected humans and animals. Protein arrays have recently been used to characterize antibody reactivity profiles of *Plasmodium* infection (Sundaresh et al. 2006; Gray et al. 2007; Doolan et al. 2008; Chen et al. 2010a; Crompton et al. 2010).

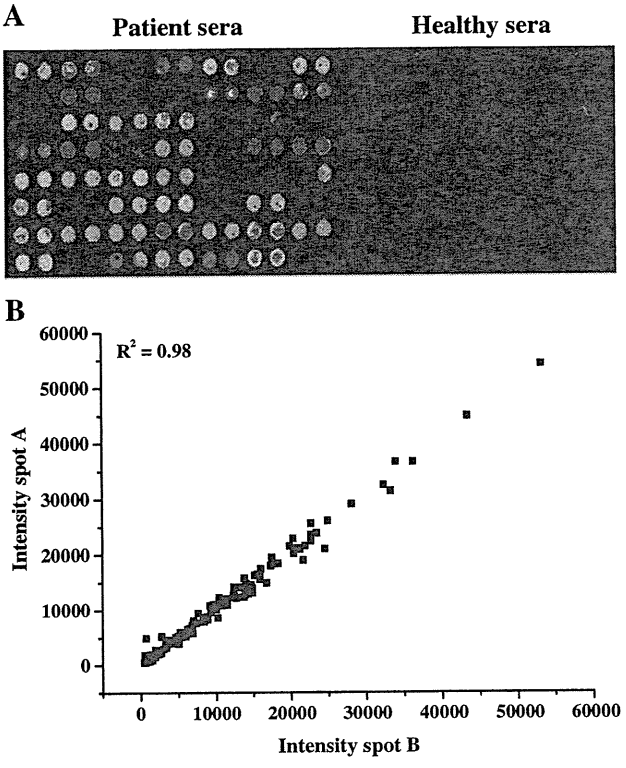

Fig. 4 Correlation between ELISA and protein arrays for antibody profiling. The ELISA absorbance readings for antibody responses against PvMSP1-19 in 130 sera samples from *P. vivax*-infected patients were compared to fluorescence measured by protein arrays. Protein array platform for profiling antibody responses to crude PvMSP1-42. **a** Crude recombinant PvMSP1-42 reacted with individual serum samples. **b** Correlation between relative spot intensities of duplicates (*spot a* versus its duplicate *spot b*)

P. vivax MSP1 is a polymorphic protein that is abundantly expressed on the merozoite surface. A processing mechanism may generate the C-terminal region of MSP1 (PvMSP1-19), which remains on the parasite surface where it appears to be essential for merozoite invasion (Cowman and Crabb 2006). PvMSP1-19 is normally purified from inclusion bodies using an *Escherichia coli* expression system (Rodrigues et al. 2005; Mehrizi et al. 2009). In the present study, the wheat germ cell-free-expressed PvMSP1-19 was purified from soluble fractions and showed positive reactivity with serum from humans naturally exposed to vivax malaria in the Republic of Korea. The antibody reactivities in this study were consistent with previously published results (Rodrigues et al. 2005; Mehrizi et al. 2009). Thus, these results indicate the proper immunogenicity of *P. vivax* proteins expressed using the wheat germ cell-free system.

We developed a protein array platform for immunoprofiling *P. vivax* infection. The concentration used for protein arrays (40 ng/spot) was five-fold lower than that for the ELISA (200 ng/well). This difference in concentrations is quite important to reduce the amount of coating antigen. Moreover, the amount of serum sample (1:200 dilution, 1 μl) used for protein arrays was 200-fold lower than that used for ELISA (1:200 dilution, 200 μl). This is a critical point for saving the amount of serum sample in the proteome-wide analysis of immune responses to infectious diseases (Felgner et al. 2009; Crompton et al. 2010).

We used protein arrays to characterize antibody reactivity profiles of *P. vivax* infection. From 230 sera samples of *P. vivax*-infected patients and healthy individuals confirmed by ELISA, protein arrays detected *P. vivax* in 112 of 130 (86.2%) microscopically confirmed positive samples. These results are consistent with the ELISA results, and the IgG frequency is consistent with previous reports in South Korea and Iran (Park et al. 2001; Mehrizi et al. 2009). Similar to the ELISA results, two false positives among 100 sera samples from healthy subjects were obtained using protein arrays. When we compared the results obtained by protein array and ELISA, the Kappa values represented excellent agreement for the recombinant PvMSP1-19 protein against sera samples

(Kappa=0.904 and total agreement=95.2%). These results validate the protein arrays for profiling antibody responses to *P. vivax* infection.

In contrast with the use of nitrocellulose-coated glass slides in previous studies (Davies et al. 2005; Doolan et al. 2008; Crompton et al. 2010), we used Ni^{2+}-chelated surface slides for in situ binding and purification of His-tagged recombinant proteins. When we analyzed the antibody response to crude PvMSP1-42 using Ni^{2+}-chelated surface slides, it has the similar fluorescent intensity in comparison with purified PvMSP1-19 in the positive sera samples. These slides are especially powerful for coating with unpurified cell-free synthesized His-tagged proteins (data not shown). These slides have two major advantages for use with protein arrays. On one hand, it is possible to avoid the majority of printed protein (99%) derived from the lysate itself, which can compete with the expressed antigen for binding to the array surface. Higher background signals may be observed by cross-reacting serum antibodies to spotted lysate proteins on nitrocellulose-coated glass slides directly (Davies et al. 2005). On the other hand, tagged proteins are bound to the Ni^{2+}-chelated surface in a uniform orientation and are not denatured. This means that they remain in the conformationally active form, thus providing optimal presentation to antibodies.

Analysis of serum reactivity profiles using protein arrays offers an opportunity to assess antibody responses against malarial antigens in a high-throughput manner. Furthermore, the novel protein array platform may be useful for profiling naturally acquired humoral immune responses to *P. vivax* infection.

Acknowledgments This work was supported by a Korean Science and Engineering Foundation (KOSEF) grant funded by the Korea Government (MOST) (No. R01-2007-000-11260-0) and National Research Foundation of Korea Grant funded by the Korean Government (2009-0075103). This work was also supported in part by grants-in-aid from the Ministry of Health, Labour and Welfare, Japan (H20-shinkou-ippan-013 and H21-chikyukibo-ippan-005), and in part by grants-in-aid from the Ministry of Education, Culture, Sports, Science and Technology, Japan (21022034). We thank Kana Kato, Rie Sekito, Mai Tasaka and Miyuki Yano for their technical assistance.

References

Aguiar JC, LaBaer J, Blair PL, Shamailova VY, Koundinya M, Russell JA, Huang F, Mar W, Anthony RM, Witney A, Caruana SR, Brizuela L, Sacci JB Jr, Hoffman SL, Carucci DJ (2004) High-throughput generation of *P. falciparum* functional molecules by recombinational cloning. Genome Res 14:2076–2082

Beare PA, Chen C, Bouman T, Pablo J, Unal B, Cockrell DC, Brown WC, Barbian KD, Porcella SF, Samuel JE, Felgner PL, Heinzen RA (2008) Candidate antigens for Q fever serodiagnosis revealed by immunoscreening of a *Coxiella burnetii* protein microarray. Clin Vaccine Immunol 15:1771–1779

Chen JH, Jung JW, Wang Y, Ha KS, Lu F, Lim CS, Takeo S, Tsuboi T, Han ET (2010a) Immunoproteomics profiling of blood stage *Plasmodium vivax* infection by high-throughput screening assays. J Proteome Res 9:6479–6489

Chen JH, Lu F, Lim CS, Kim JY, Ahn HJ, Suh IB, Takeo S, Tsuboi T, Sattabongkot J, Han ET (2010b) Detection of *Plasmodium vivax* infection in the Republic of Korea by loop-mediated isothermal amplification (LAMP). Acta Trop 113:61–65

Collins WE, Kaslow DC, Sullivan JS, Morris CL, Galland GG, Yang C, Saekhou AM, Xiao L, Lal AA (1999) Testing the efficacy of a recombinant merozoite surface protein MSP-1 (19) of *Plasmodium vivax* in *Saimiri boliviensis* monkeys. Am J Trop Med Hyg 60:350–356

Cowman AF, Crabb BS (2006) Invasion of red blood cells by malaria parasites. Cell 124:755–766

Crompton PD, Kayala MA, Traore B, Kayentao K, Ongoiba A, Weiss GE, Molina DM, Burk CR, Waisberg M, Jasinskas A, Tan X, Doumbo S, Doumtabe D, Kone Y, Narum DL, Liang X, Doumbo OK, Miller LH, Doolan DL, Baldi P, Felgner PL, Pierce SK (2010) A prospective analysis of the Ab response to *Plasmodium falciparum* before and after a malaria season by protein microarray. Proc Natl Acad Sci USA 107:6958–6963

Cunha MG, Rodrigues MM, Soares IS (2001) Comparison of the immunogenic properties of recombinant proteins representing the *Plasmodium vivax* vaccine candidate MSP1(19) expressed in distinct bacterial vectors. Vaccine 20:385–396

Davies DH, Liang X, Hernandez JE, Randall A, Hirst S, Mu Y, Romero KM, Nguyen TT, Kalantari-Dehaghi M, Crotty S, Baldi P, Villarreal LP, Felgner PL (2005) Profiling the humoral immune response to infection by using proteome microarrays: high-throughput vaccine and diagnostic antigen discovery. Proc Natl Acad Sci USA 102:547–552

Davies DH, Molina DM, Wrammert J, Miller J, Hirst S, Mu Y, Pablo J, Unal B, Nakajima-Sasaki R, Liang X, Crotty S, Karem KL, Damon IK, Ahmed R, Villarreal L, Felgner PL (2007) Proteome-wide analysis of the serological response to vaccinia and smallpox. Proteomics 7:1678–1686

Davies DH, Wyatt LS, Newman FK, Earl PL, Chun S, Hernandez JE, Molina DM, Hirst S, Moss B, Frey SE, Felgner PL (2008) Antibody profiling by proteome microarray reveals the immunogenicity of the attenuated smallpox vaccine modified vaccinia virus ankara is comparable to that of Dryvax. J Virol 82:652–663

Doolan DL, Mu Y, Unal B, Sundaresh S, Hirst S, Valdez C, Randall A, Molina D, Liang X, Freilich DA, Oloo JA, Blair PL, Aguiar JC, Baldi P, Davies DH, Felgner PL (2008) Profiling humoral immune responses to *P. falciparum* infection with protein microarrays. Proteomics 8:4680–4694

Felgner PL, Kayala MA, Vigil A, Burk C, Nakajima-Sasaki R, Pablo J, Molina DM, Hirst S, Chew JS, Wang D, Tan G, Duffield M, Yang R, Neel J, Chantratita N, Bancroft G, Lertmemongkolchai G, Davies DH, Baldi P, Peacock S, Titball RW (2009) A *Burkholderia pseudomallei* protein microarray reveals serodiagnostic and cross-reactive antigens. Proc Natl Acad Sci USA 106:13499–13504

Fernandez-Becerra C, Sanz S, Brucet M, Stanisic DI, Alves FP, Camargo EP, Alonso PL, Mueller I, del Portillo HA (2010) Naturally acquired humoral immune responses against the N- and C-termini of the *Plasmodium vivax* MSP1 protein in endemic regions of Brazil and Papua New Guinea using a multiplex assay. Malar J 9:29

Gardner MJ, Hall N, Fung E, White O, Berriman M, Hyman RW, Carlton JM, Pain A, Nelson KE, Bowman S, Paulsen IT, James K, Eisen JA, Rutherford K, Salzberg SL, Craig A, Kyes S, Chan MS, Nene V, Shallom SJ, Suh B, Peterson J, Angiuoli S, Pertea M, Allen J, Selengut J, Haft D, Mather MW, Vaidya AB, Martin DM, Fairlamb AH, Fraunholz MJ, Roos DS, Ralph SA,

McFadden GI, Cummings LM, Subramanian GM, Mungall C, Venter JC, Carucci DJ, Hoffman SL, Newbold C, Davis RW, Fraser CM, Barrell B (2002) Genome sequence of the human malaria parasite *Plasmodium falciparum*. Nature 419:498–511

Gray JC, Corran PH, Mangia E, Gaunt MW, Li Q, Tetteh KK, Polley SD, Conway DJ, Holder AA, Bacarese-Hamilton T, Riley EM, Crisanti A (2007) Profiling the antibody immune response against blood stage malaria vaccine candidates. Clin Chem 53:1244–1253

Langhorne J, Ndungu FM, Sponaas AM, Marsh K (2008) Immunity to malaria: more questions than answers. Nat Immunol 9:725–732

Mehrizi AA, Zakeri S, Salmanian AH, Sanati MH, Djadid ND (2009) IgG subclasses pattern and high-avidity antibody to the C-terminal region of merozoite surface protein 1 of *Plasmodium vivax* in an unstable hypoendemic region in Iran. Acta Trop 112:1–7

Mezzasoma L, Bacarese-Hamilton T, Di Cristina M, Rossi R, Bistoni F, Crisanti A (2002) Antigen microarrays for serodiagnosis of infectious diseases. Clin Chem 48:121–130

Mueller I, Galinski MR, Baird JK, Carlton JM, Kochar DK, Alonso PL, del Portillo HA (2009) Key gaps in the knowledge of *Plasmodium vivax*, a neglected human malaria parasite. Lancet Infect Dis 9:555–566

Parekh FK, Richie TL (2007) Characterization of immune reactivity profiles using microarray technology may expedite identification of candidate antigens for next generation malaria vaccines. Clin Chem 53:1183–1185

Park JW, Moon SH, Yeom JS, Lim KJ, Sohn MJ, Jung WC, Cho YJ, Jeon KW, Ju W, Ki CS, Oh MD, Choe K (2001) Naturally acquired antibody responses to the C-terminal region of merozoite surface protein 1 of *Plasmodium vivax* in Korea. Clin Diagn Lab Immunol 8:14–20

Park JY, Jung SH, Jung JW, Kwon MH, Yoo JO, Kim YM, Ha KS (2009) A novel array-based assay of in situ tissue transglutaminase activity in human umbilical vein endothelial cells. Anal Biochem 394:217–222

Perera KL, Handunnetti SM, Holm I, Longacre S, Mendis K (1998) Baculovirus merozoite surface protein 1 C-terminal recombinant antigens are highly protective in a natural primate model for human *Plasmodium vivax* malaria. Infect Immun 66:1500–1506

Price RN, Tjitra E, Guerra CA, Yeung S, White NJ, Anstey NM (2007) Vivax malaria: neglected and not benign. Am J Trop Med Hyg 77:79–87

Richie TL, Saul A (2002) Progress and challenges for malaria vaccines. Nature 415:694–701

Rodrigues MH, Rodrigues KM, Oliveira TR, Comodo AN, Rodrigues MM, Kocken CH, Thomas AW, Soares IS (2005) Antibody response of naturally infected individuals to recombinant *Plasmodium vivax* apical membrane antigen-1. Int J Parasitol 35:185–192

Sachdeva S, Ahmad G, Malhotra P, Mukherjee P, Chauhan VS (2004) Comparison of immunogenicities of recombinant *Plasmodium vivax* merozoite surface protein 1 19- and 42-kiloDalton fragments expressed in *Escherichia coli*. Infect Immun 72:5775–5782

Steller S, Angenendt P, Cahill DJ, Heuberger S, Lehrach H, Kreutzberger J (2005) Bacterial protein microarrays for identification of new potential diagnostic markers for *Neisseria meningitidis* infections. Proteomics 5:2048–2055

Sundaresh S, Doolan DL, Hirst S, Mu Y, Unal B, Davies DH, Felgner PL, Baldi P (2006) Identification of humoral immune responses in protein microarrays using DNA microarray data analysis techniques. Bioinformatics 22:1760–1766

Tsuboi T, Takeo S, Iriko H, Jin L, Tsuchimochi M, Matsuda S, Han ET, Otsuki H, Kaneko O, Sattabongkot J, Udomsangpetch R, Sawasaki T, Torii M, Endo Y (2008) Wheat germ cell-free system-based production of malaria proteins for discovery of novel vaccine candidates. Infect Immun 76:1702–1708

Wickramarachchi T, Illeperuma RJ, Perera L, Bandara S, Holm I, Longacre S, Handunnetti SM, Udagama-Randeniya PV (2007) Comparison of naturally acquired antibody responses against the C-terminal processing products of *Plasmodium vivax* Merozoite Surface Protein-1 under low transmission and unstable malaria conditions in Sri Lanka. Int J Parasitol 37:199–208

Zeyrek FY, Babaoglu A, Demirel S, Erdogan DD, Ak M, Korkmaz M, Coban C (2008) Analysis of naturally acquired antibody responses to the 19-kd C-terminal region of merozoite surface protein-1 of *Plasmodium vivax* from individuals in Sanliurfa, Turkey. Am J Trop Med Hyg 78:729–732

Zhu H, Hu S, Jona G, Zhu X, Kreiswirth N, Willey BM, Mazzulli T, Liu G, Song Q, Chen P, Cameron M, Tyler A, Wang J, Wen J, Chen W, Compton S, Snyder M (2006) Severe acute respiratory syndrome diagnostics using a coronavirus protein microarray. Proc Natl Acad Sci USA 103:4011–4016